Colloquium: Modeling friction: From nanoscale to mesoscale

Andrea Vanossi

CNR-IOM Democritos National Simulation Center, Via Bonomea 265, 34136 Trieste, Italy and International School for Advanced Studies (SISSA), Via Bonomea 265, 34136 Trieste, Italy

Nicola Manini

Dipartimento di Fisica, Università degli Studi di Milano, Via Celoria 16, 20133 Milano, Italy and International School for Advanced Studies (SISSA), Via Bonomea 265, 34136 Trieste, Italy

Michael Urbakh

School of Chemistry, Tel Aviv University, 69978 Tel Aviv, Israel

Stefano Zapperi

CNR-IENI, Via R. Cozzi 53, 20125 Milano, Italy and ISI Foundation, Via Alassio 11C, 10126 Torino, Italy

Erio Tosatti

International School for Advanced Studies (SISSA), Via Bonomea 265, 34136 Trieste, Italy, CNR-IOM Democritos National Simulation Center, Via Bonomea 265, 34136 Trieste, Italy, and International Center for Theoretical Physics (ICTP), Strada Costiera 11, 34151 Trieste, Italy

(published 2 April 2013)

The physics of sliding friction is gaining impulse from nanoscale and mesoscale experiments, simulations, and theoretical modeling. This Colloquium reviews some recent developments in modeling and in atomistic simulation of friction, covering open-ended directions, unconventional nanofrictional systems, and unsolved problems.

CONTENTS

I. INTRODUCTION

Frictional motion plays a central role in diverse systems and phenomena that span vast ranges of scales, from the nanometer contacts inherent in micromachines and nanomachines (Urbakh *et al.*, 2004) and biological molecular motors (Bormuth *et al.*, 2009) to the geophysical scales characteristic of earthquakes (Scholz, 1998). Because of its enormous practical and technological importance, the friction problem has stimulated progress over the centuries. Historical figures from Leonardo da Vinci onward have brought friction into the field of physics, with the formulation of time-honored phenomenological frictional laws, which have been referred to as the Coulomb-Amontons laws. These statements can be briefly summarized as follows: (i) frictional force is independent of the apparent area of contact, (ii) frictional force is proportional to the normal load, and (iii) kinetic friction (the force to keep relative motion at constant speed) does not depend on the sliding velocity and is smaller than static friction (the force needed to initiate motion between two contacting bodies at rest). Also in the light of a mass of empirical data, serious

attempts were made in the first half of the 20th century toward a microscopic understanding of these laws (Bowden and Tabor, 1950). Whereas the basic physics underlying sliding friction—nonequilibrium statistical mechanics of solids, sheared fluids, and moving surfaces—is in principle quite exciting, the field as a whole has (with notable exceptions) failed to attract adequate interest by the physicist until the last few decades. A lack of microscopic data, and a corresponding lack of theory, have perhaps contributed to project an unattractive image of sliding friction.

Three quiet revolutions, of broad nature and unrelated to friction, are radically changing this state of affairs. First, progress in the general area of complexity provided new tools to tackle nonequilibrium disordered systems with interacting degrees of freedom. Second, and crucially, the developments in nanotechnology extended the study of friction and permitted its analysis on well-characterized materials and surfaces at the nanoscale and microscale. Notably the invention of scanning tip instruments of the atomic force microscope (AFM) family (Binnig, Quate, and Gerber, 1986) has opened *nanofriction* as a brand new avenue; the use of the surface force apparatus (SFA) (Israelachvili, 1992) led to the systematic studies of confined mesoscopic systems under shear; while instruments such as the quartz crystal microbalance (QCM) (Krim and Widom, 1988; Krim, 1996) measure the inertial sliding friction of adsorbate submonolayers. Thanks to these methods, a mass of fresh data and information on well-defined systems, surfaces, materials, and physical conditions has accumulated in the last two decades (Carpick and Salmeron, 1997). The resulting insights into the atomic size contacts themselves in terms of chemical interactions and of the elementary processes that are involved in the excitation and dissipation of energy are changing our perspective. Third, computer simulations have had a strong boost, also allowed by the fantastic growth of computer power. The numerical study of frictional models on the one hand, and direct atomistic molecular dynamics simulations, on the other hand, are jointly advancing our theoretical understanding. Invaluable initial reviews of the progress brought about by these revolutions in our physical understanding of sliding friction can be found in Persson (2000a) and Mate (2008).

Despite the practical and fundamental importance of friction and the growing efforts in the field, many key aspects of the dynamics of friction are not yet well understood. Even for the most studied nanoscale systems, such as AFM sliding on graphite or NaCl surfaces, a microscopic mechanism of friction is still lacking, and experimental observations (for instance, velocity and temperature dependencies of friction) have been rationalized within simplified models including empirical parameters (Riedo *et al.*, 2003; Jansen *et al.*, 2010; Barel *et al.*, 2011). Fundamental theory is still difficult in all fields of sliding friction, including nanofriction, because the sliding motion generally involves sudden nonlinear stick-slip events that cannot be treated within traditional theoretical approaches such as linear-response theory and hydrodynamics. Experiments in tribology have long suffered from the inability to directly observe what takes place at a sliding interface. Although AFM, SFA, and QCM techniques have identified many friction phenomena at the nanoscale, many interpretative pitfalls still result from indirect or *ex situ*

characterization of contact surfaces. In this colloquium we cover some aspects, progress, and problems in the current modeling and simulation of sliding friction, from nanoscale to mesoscale. In nanoscale friction, we consider systems that are small enough to be treated at the atomistic scale, such as in the AFM experiments. For larger systems, we need a mesoscopic approach that lies in between the atomistic details and the macroscopic behavior. In the spirit of a colloquium we intend to draw examples from our own experience to illustrate some of the concepts and points of interest, growth, and doubt in selected forefront areas.

One of the main difficulties in understanding and predicting frictional response is the intrinsic complexity of highly nonequilibrium processes going on in any tribological contact, which include detachment and reattachment of multiple microscopic junctions (bonds) between the surfaces in relative motion while still in contact (Gerde and Marder, 2001; Urbakh *et al.*, 2004; Bormuth *et al.*, 2009). Therefore friction is intimately related to instabilities that occur on a local microscopic scale, inducing an occasional fast motion of the corresponding degrees of freedom even if the slider's center-of-mass velocity is extremely small. Understanding the physical nature of these instabilities is crucial for the elucidation of the mechanism of friction, as we emphasize below.

Sliding friction has been addressed following different types of theoretical approaches: "minimalistic" models (MM), atomistic molecular dynamics (MD) simulations, mesoscopic multicontact models, and phenomenological rate-state (RS) models.

MMs are discussed in Sec. II. They provide an intermediate level description between atomic scale physics and macroscopic phenomenological approaches like RS models, focusing on a small number of relevant degrees of freedom which describe the sliding motion, and exhibit instabilities during stick slip. Applications of MMs provided explanations for phenomena of high complexity [see, e.g., Müser, Urbakh, and Robbins (2003) and Vanossi and Braun (2007)]. On the whole, MMs are playing a major role in rationalizing the wealth of nanoscale and mesoscale friction data produced over the last decades.

Atomistic MD simulations, discussed in Sec. III, have a wide range of applicability in nanoscale friction, and have reached a high level of rigor and accuracy (Robbins and Müser, 2001). But, as discussed in Sec. III.B, they are mostly limited to time and length scales which are too short to emulate many tribological phenomena. An important issue, therefore, is how to reduce the large-scale, many-parameter MD equations to simpler mesoscale descriptions based on fewer degrees of freedom.

Multicontact models, discussed in Sec. IV, provide such a simplified description in terms of dynamical formation and rupture of elastically coupled contacts. At the largest macroscopic scale, phenomenological RS models simplify the description even further, introducing one or two dynamical equations with coefficients chosen to fit experimental quantities and then used to describe a wide range of observed frictional behavior, such as the transition between stick slip (regular or chaotic) and smooth sliding (Carlson and Batista, 1996), and variations of friction for a sudden change of velocity (Dietrich, 1979; Ruina, 1983). RS models are often

the best available approaches to describe macroscopic friction in the ordinary world, from the microsize (Baumberger, Berthoud, and Caroli, 1999) to larger and larger scales (Scholz, 1998). However, most of the "state variables" in RS models cannot be easily related to physical system properties, a fact that limits the insight and predictive power of these models. This Colloquium is limited to nanoscale and mesoscale frictional modeling, and will not further deal with RS models; the latter are well covered, for example, by Marone (1998). Instead, Sec. V will present theoretical case studies with model descriptions of a few examples of nanofrictional phenomena, such as electronic friction, magnetic dissipation, carbon nanotube tribology, and friction in colloidal systems. For a closer and fresh perception of where the field stands, we also include a partial and incomplete list of problems that, in our perspective, still stand out for future theoretical study in friction and nanofriction.

II. SIMPLE NANOFRICTIONAL MODELS

A. The Prandtl-Tomlinson model

The Prandtl-Tomlinson (PT) model (Prandtl, 1928; Tomlinson, 1929), which we discuss here in some detail, is the most successful and influential MM so far suggested for description of nanoscale friction. In particular, it addresses friction force microscopy (FFM), where friction forces are measured by dragging an AFM tip along a surface. Qualitative conclusions drawn with this model provide guidance to understanding friction at the nanoscale and often retain their validity in more advanced models and MD simulations.

The PT model assumes that a point mass m (mimicking, e.g., the AFM tip) is dragged over a one-dimensional sinusoidal potential representing the interaction between the tip and a crystalline substrate. The point tip is pulled by a spring of effective elastic constant K, extending between the tip position x and the position of the microscope support stage, that is driven with a constant velocity v relative to the substrate; see Fig. 1(a). Thus the total potential experienced by the tip consists of two parts: (i) the tip-substrate interaction and (ii) the elastic interaction between the tip and the support, and can be written as

$$U(x, t) = U_0 \cos\left(\frac{2\pi}{a} x\right) + \frac{K}{2}(x - vt)^2, \qquad (1)$$

where U_0 is the amplitude and a is the periodicity of the tip-substrate potential. Note that in an AFM experiment the real "spring constant" mimicked by K in the PT model is not only due to the torsional stiffness of the cantilever but also includes the contribution from the lateral stiffness of the contact. There is no attempt in the model to describe realistically the energy dissipation into the substrate (Joule heat) and all dissipation is described by a viscouslike force $-m\gamma\dot{x}$, where γ is a damping coefficient. The instantaneous lateral friction force measured in FFM experiments reads $F = -K(x - vt)$, and the kinetic friction F_k is the time average of F.

The PT model predicts two different modes for the tip motion, depending on the dimensionless parameter $\eta = 4\pi^2 U_0/Ka^2$, which represents the ratio between the stiffnesses of the tip-substrate potential and the pulling spring.
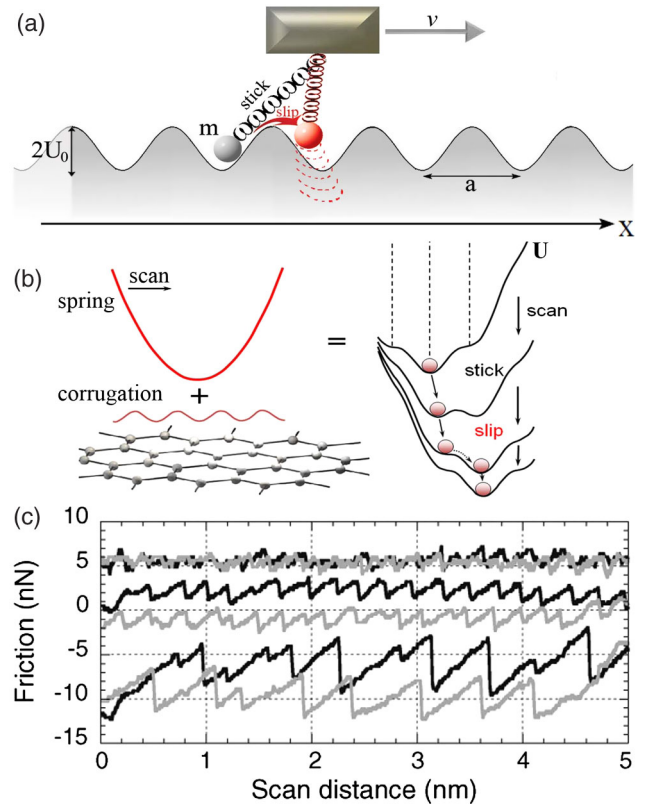

FIG. 1 (color online). Stick-slip in (a) a cartoon of the PT model, (b) energy landscape for a soft spring (low K). The total potential (harmonic spring + sinusoidal substrate) exhibits different metastable minima, giving rise to the stick-slip behavior, and (c) a representative experimental friction pattern, for increasing load. Lateral force vs position traces demonstrate transitions from smooth sliding (top) to single (middle) and mostly double slips (bottom). Similar patterns can be generated within the PT model. From Medyanik *et al.*, 2006.

When $\eta < 1$, the total potential $U(x)$ exhibits only one minimum and the time-dependent sliding motion is smooth; for $\eta > 1$, two or more minima appear in $U(x)$, and the sliding is discontinuous, characterized by stick-slip transitions; see Fig. 1(b). The value $\eta = 1$ represents the transition from smooth sliding to slips by one lattice site (single-slip regime).

Physically, stick-slip motion corresponds to jumps of the tip between successive minima of $U(x)$, due to instabilities induced by the driving spring ($\partial U/\partial x = 0$, $\partial^2 U/\partial x^2 = 0$). Close to the inflection point the height of the barrier preventing the tip sliding decreases with the applied force, as $\Delta E \propto$ (const $- F)^{3/2}$ (Sang, Dubé, and Grant, 2001; Dudko *et al.*, 2002; Maloney and Lacks, 2006) This type of externally induced topological change in a free-energy landscape is known as a fold catastrophe, and it has been found in many driven systems, including superconducting quantum interference devices (Kurkijarvi, 1972; Garg, 1995), mechanically deformed glasses (Johnson and Samwer, 2005), and stretched proteins (Berkovich *et al.*, 2010; Lacks, Willis, and Robinson, 2010). The simulation results obtained for diverse systems show that the fold-catastrophe scaling is in fact accurate not only in the immediate vicinity of the inflection point but over reasonably large intervals of loads.

The possibility of slips of higher multiplicity (multiple-slip regime) occurs for larger values of $\eta > 4.604$ (Medyanik *et al.*, 2006). It should be noted that this is a necessary but not sufficient condition to observe multiple slips, since the observed dynamics depends also on the damping coefficient γ. In particular, for $\eta > 4.604$ one can distinguish between the overdamped regime of motion, $\gamma > \sqrt{U_0/m}4\pi/a$, where the tip jumps between nearest-neighbor minima of the potential, and the underdamped regime, $\gamma < \sqrt{U_0/m}4\pi/a$, where the tip may perform multiple slips over a number of lattice sites and even overshoot the lowest well of the potential $U(x)$. In that case, the minimal spring force reached during stick-slip oscillations is negative.

The elastic instability occurring for $\eta > 1$ results in a nonzero value of the low-velocity kinetic friction that is given by the energy drop from the point of instability to the next minimum of the potential divided by a (Helman, Baltensperger, and Holyst, 1994). For $\eta < 1$, this instability does not exist, friction is viscous, and $F_k \rightarrow 0$ for $v \rightarrow 0$. The emergence of static friction can be interpreted as the arousal of a saddle-node bifurcation as a function of η, realizing a sort of fold-catastrophe scenario (Gilmore, 1981).

Note that in real systems, at finite temperature, hysteresis and dissipation must always disappear in the zero-speed limit of adiabatic sliding, where stick-slip instabilities are preempted by thermal fluctuations. This regime, sometimes termed thermolubricity, is addressed in Sec. II.C, particularly by Eq. (4).

In experiments, the effective value of the PT parameter η can be controlled by the variation of the normal load on the contact, which changes the potential corrugation U_0 more than the contact stiffness. FFM experiments at low normal loads indeed demonstrated smooth sliding with ultralow friction, connected to the absence of elastic instabilities (Socoliuc *et al.*, 2004; Medyanik *et al.*, 2006). At higher loads, ''atomic'' stick-slip took place with the atomic periodicity of the substrate lattice, while increasing load (corresponding to increasing U_0) further led to a multiple-slip regime as predicted by the PT model; see Fig. 1(c).

B. Extensions of the Prandtl-Tomlinson model

Several generalizations of the original, one-dimensional PT model have marked new steps toward understanding and implementation of frictional phenomena. These extensions included considerations of the following:

- the two-dimensional structure of surfaces that led to the introduction of frictional imaging of interfaces (Gyalog *et al.*, 1995; Prioli *et al.*, 2003; Fusco and Fasolino, 2004, 2005);
- thermal fluctuations that allowed us to understand an origin of velocity dependence of friction and introduced a new regime of friction, named thermolubricity (Gnecco *et al.*, 2000; Sang, Dubé, and Grant, 2001; Dudko *et al.*, 2002; Riedo *et al.*, 2003; Reimann and Evstigneev, 2004; Krylov *et al.*, 2005);
- coupling between normal and lateral motion of the slider (Rozman, Urbakh, and Klafter, 1998; Zaloj, Urbakh, and Klafter, 1999) that led to a new approach to control friction and wear by modulating the normal

load (Socoliuc *et al.*, 2006; Lantz, Wiesmann, and Gotsmann, 2009); and

- flexibility of the AFM tip apex that led to a predictions of new regimes of motion exhibiting complex stick-slip patterns (Krylov *et al.*, 2006; Tshiprut, Filippov, and Urbakh, 2008).

Deferring some of these points bearing contact with the Frenkel-Kontorova model, we focus first on the effect of temperature on friction.

C. Thermal and velocity effects on nanoscale friction

The main aspects of thermal effects on friction were considered in the pioneering work by Prandtl (1928). Thermal effects can be incorporated into the model (1) by adding a thermal random force $\hat{f}(t)$ to the conservative force between the slider and substrate and the damping term $-m\gamma\dot{x}$. Then the tip motion is described by the following Langevin equation:

$$m\ddot{x} + m\gamma\dot{x} = -\frac{\partial U(x,t)}{\partial x} + \hat{f}(t). \qquad (2)$$

The random force should satisfy the fluctuation-dissipation theorem; as usual, it is chosen with zero mean $\langle \hat{f}(t) \rangle = 0$ and δ correlated,

$$\langle \hat{f}(t)f(t') \rangle = 2m\gamma k_B T \delta(t - t'), \qquad (3)$$

where k_B denotes the Boltzmann constant and T is temperature. The random forces and the damping term arise from interactions with phonons and/or other fast excitations that are not treated explicitly.

In the thermal PT model, Eqs. (2) and (3), beside the PT parameter η, thermal fluctuations bring out a new dimensionless parameter Δ representing the ratio between the pulling rate v/a and the characteristic rate of thermally activated jumps over the potential barriers, $\omega_0 \exp(-U_0/k_B T)$, where ω_0 is the attempt frequency (Krylov *et al.*, 2005). As a result, one should distinguish between two regimes of motion: (i) $\Delta \ll 1$, the regime of very low velocities or high temperatures (typically $v < 1$ nm/s at room temperature), where the tip has enough time to jump back and forth across the barrier; and (ii) $\Delta \gg 1$, the stick-slip regime of motion, where thermal fluctuations only occasionally assist the tip to cross the barrier before the elastic instability is reached. In these two regimes, the following expressions for kinetic friction have been suggested (Sang, Dubé, and Grant, 2001; Dudko *et al.*, 2002; Krylov *et al.*, 2005):

$$F_k(v, T) = \alpha(T)v + O(v^3), \qquad \Delta \ll 1, \qquad (4)$$

$$F_k(v, T) = F_0 - bT^{2/3}\ln^{2/3}\left(B\frac{T}{v}\right), \qquad (5)$$

$$\Delta \gg 1 \quad \text{and} \quad v < BT.$$

Here F_0 is the athermal ($T = 0$) low-velocity limit of friction, $\alpha(T) \propto (K/\omega_0)(U_0/k_B T)\exp(U_0/k_B T)$ is the equilibrium damping felt by the tip that is independent of the ad hoc damping coefficient γ, and b, B are positive constants which depend on m, K, a, U_0, and γ but not on v and T. Equation (4), describing the slow friction regime called

thermolubricity (Krylov *et al.*, 2005), corresponds to the linear-response regime, while Eq. (5) has been derived assuming that thermally activated depinning still occurs in the vicinity of the athermal instability point. The velocity and temperature dependencies of friction force predicted by Eq. (5) result from the fold-catastrophe scaling of the potential barriers, $\Delta E \propto (\mathrm{const} - F)^{3/2}$, which was discussed in Sec. II.A. Furthermore, in between the two regimes described by Eqs. (4) and (5) one should observe a logarithmic dependence of F_k on velocity. However, it is difficult to distinguish between $[\ln(v)]^{2/3}$ and simple $\ln(v)$ behavior in experiments and numerical simulations (Müser, 2011). The logarithmic (or $[\ln(v)]^{2/3}$) regime tends to span many decades, until v becomes so large that the inertial or viscouslike effects set in. The $[\ln(v)]^{2/3}$ dependence of the average rupture force has been also found in single-molecule unbinding experiments, where the energy landscape of complex biomolecules is probed by applying time-dependent forces (Dudko *et al.*, 2003).

The theoretical framework outlined above has explained a number of FFM experimental results on single crystal surfaces (Gnecco *et al.*, 2000; Riedo *et al.*, 2003; Stills and Overney, 2003). Furthermore, the statistical distribution of friction forces was measured to match predictions from the PT model (Schirmeisen, Jansen, and Fuchs, 2005). These results provide strong evidence that atomic stick-slip motion in FFM is attributable to thermally activated slip out of a local minimum as described by the PT model. Thermally activated stick-slip friction is only seen in MD at sufficiently low speeds, which are so far only achievable through accelerated MD (Li, Dong *et al.*, 2011). At higher speeds, friction is mostly determined by dissipative athermal dynamical processes, which correspond to a fundamentally different regime of sliding. This severely limits the regime of validity of comparisons of the PT model with MD simulations.

Equations (4) and (5) also predict that kinetic friction should decrease with increasing temperature (Sang, Dubé, and Grant, 2001; Dudko *et al.*, 2002; Steiner *et al.*, 2009). Thermal excitations in fact help overcome energy barriers and reduce the stick-slip jump magnitude, so that nanofriction should decrease with temperature provided no other surface or material parameters are altered by temperature (Szlufarska, Chandross, and Carpick, 2008). Up to now, most FFM measurements have been performed at room temperature, so that the temperature dependence of nanoscale friction has rarely been addressed in experimental work. Recent experimental results (Schirmeisen *et al.*, 2006; Zhao *et al.*, 2009; Barel *et al.*, 2010a, 2010b), however, strongly disagree with the predictions of Eqs. (4) and (5). Friction forces exhibit a peak at cryogenic temperatures for different classes of materials, including amorphous, crystalline, and layered surfaces. Can this effect be explained within the PT model? Recent analysis of the thermal PT model (Tshiprut, Zelner, and Urbakh, 2009; Fajardo and Mazo, 2010) demonstrated that the friction force may indeed exhibit a peak in the interval of temperatures corresponding to a transition from a multiple-slip regime of motion, at low T, to the single-slip regime at higher T. In this picture, interplay between thermally activated jumps over potential barriers and the reduction of the slip spatial extension with T may lead to a nonmonotonic temperature dependence of friction. However,

the PT model fails to reproduce the observed features of the temperature and velocity dependencies of kinetic friction, and of the force traces measured with atomic resolution.

D. The Frenkel-Kontorova model

The basic model describing the sliding of crystalline interfaces is the one-dimensional Frenkel-Kontorova (FK) model; see Braun and Kivshar (2004) and references therein. First analytically treated by Dehlinger (1929) and then introduced to describe dislocations in solids (Frenkel and Kontorova, 1938; Kontorova and Frenkel, 1938a, 1938b), the FK model subsequently found a wide area of applications, in particular, in surface physics, where it is often used to unravel the physical behavior of adsorbed monolayers, specifically to address competing incommensurate periodicities.

The standard FK model Hamiltonian is

$$H = \sum_i \left[\frac{p_i^2}{2m} + \frac{K}{2}(x_{i+1} - x_i - a_c)^2 + \frac{U_0}{2}\cos\frac{2\pi x_i}{a_b} \right], \quad (6)$$

describing a 1D chain of N harmonically coupled classical "atoms" subjected to a sinusoidal potential; see Fig. 2. The first term in Eq. (6) is the kinetic energy of the chain, the second one describes the harmonic interaction of the nearest neighbors in the chain with elastic constant K and equilibrium distance a_c, and the last term is the interaction of the chain particles with the periodic potential of magnitude U_0 and periodicity a_b. Static friction is probed by driving all atoms with an extra adiabatically increasing force F until sliding initiates.

Tribological processes in the FK model are ruled by kink (topological soliton) excitations. Consider the simplest case of the trivial commensurate ground state when the number of atoms N coincides with the number of minima of the substrate potential M, so that the dimensionless concentration $\theta = N/M = a_b/a_c$ is 1. In this case, adding (or subtracting) one extra atom results in a chain configuration with a kink (or an antikink) excitation. After relaxation, the minimum-energy configuration corresponds to a local compression (or extension in the antikink case) of the chain. Kinks are important because they move along the chain far more easily than atoms: The activation energy for kink motion (the Peierls-Nabarro barrier) is always smaller or much smaller than the amplitude U_0 of the substrate potential. The relevance of topological defects for slip can be understood going back to the pioneering work by Frenkel on the shear strength of crystalline solids (Frenkel, 1926). Frenkel estimated the ideal plastic yield stress of a crystal as the stress needed to displace one atomic plane by one lattice spacing. This calculation leads to an estimate for
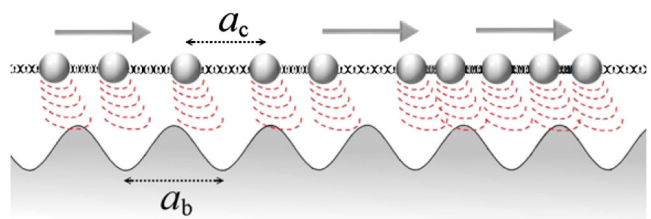

FIG. 2 (color online).   A sketch of the FK model with the two competing lengths: interparticle and substrate periodicities.

the yield stress which is of the order of the shear modulus. The result is in contradiction with experiments which typically show much smaller results. The reason for this discrepancy is rooted in the presence of dislocations which can be displaced by much smaller stresses, leading to plastic deformation much earlier than in the perfect-crystal limit. In ideal conditions, the only barrier to dislocation motion is the Peierls-Nabarro stress due to the periodic lattice and this is typically orders of magnitude smaller than the shear modulus.

Because the kinks (antikinks) correspond to extra atoms (vacancies), their motion provides a mechanism for mass transport along the chain and are thus responsible for mobility, conductivity, and diffusivity. The higher the concentration of kinks, the higher will be the system mobility (Vanossi *et al.*, 2003). When the ground state is commensurate (i.e., $\theta = 1$), at nonzero temperature, the first step to initiate motion in the FK model is the creation of a kink-antikink pair; see Fig. 3.

When the elastic layer is of finite extension, kinks are usually generated at one end of the chain and then propagate along the chain until disappearing at the other free end. Each run of the kink (antikink) through the chain results in the shift of the whole chain by one lattice constant a_b. In the case of a finite film confined between two solids, one may similarly expect that the onset of sliding is initiated by the creation of a local compression (kink, misfit dislocation) at the boundary of the contact, while kink's motion is the basic mechanism of sliding.

A crucial role in the FK model is played by incommensurability and the *Aubry transition* (Peyrard and Aubry, 1983) connected with it. Let the substrate period a_b and the natural period of the chain a_c be such that, in the limit of an infinite system's length, their ratio $\theta = a_b/a_c$ is irrational. Roughly speaking, in this case the FK chain acquires a "staircase"
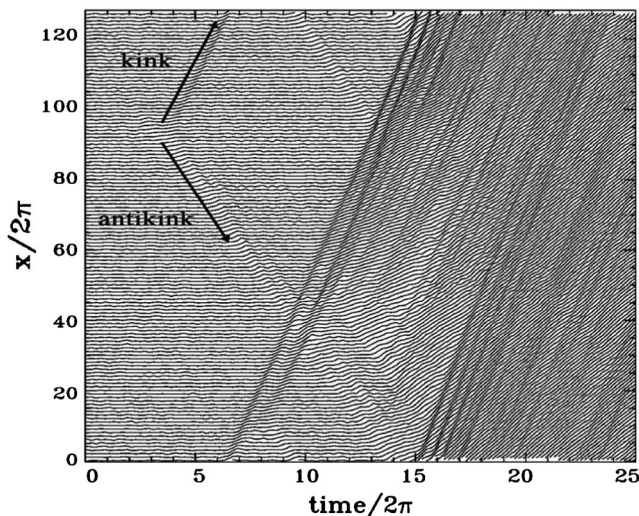

FIG. 3. Detailed behavior (atomic trajectories vs time) at the depinning transition at a small nonzero temperature of the FK chain with $\theta = 1$. The onset of motion is marked by the creation of one kink-antikink pair. The kink and antikink move in opposite directions, collide quasielastically (because of the periodic boundary conditions), and soon a second kink-antikink pair is created in the tail of the primary kink. This process repeats with an exponential (avalanche-like) growth of the kink-antikink concentration, leading to the totally sliding state. Adapted from Braun, Bishop, and Röder, 1997.

deformation, with regions of approximate commensurability separated by regularly spaced kinks (or antikinks if $\theta < 1$). If there is a nonzero probability to find particles arbitrarily close to the maximum potential energy U_0, these kinks are unpinned and mobile; otherwise they are pinned (Floria and Mazo, 1996). For a fixed amplitude of the substrate potential U_0, the FK ground state undergoes a transition between these two states (the Aubry transition) at a critical value $K = K_c$ of the chain stiffness. K_c depends dramatically and discontinuously on the incommensurability ratio a_b/a_c defining the interface. In particular, it has been proven that K_c takes the minimal possible value given by $\approx 1.029\,192\,6$ [in units of $2U_0(\pi/a_b)^2$] for the ratio equal to the irrational golden mean $a_b/a_c = (1 + \sqrt{5})/2$ (Braun and Kivshar, 2004). From a physical point of view, this means that for $K > K_c$ there is a continuum set of ground states that can be reached adiabatically by the chain through nonrigid displacements of its atoms at no energy cost (*sliding mode*). On the other hand, for $K < K_c$, the atoms are all trapped close to the minima of the substrate potential and thus require a finite energy per kink (equal to the Peierls-Nabarro barrier) to move over the corrugated substrate. Thus, for incommensurate contacts above the Aubry transition ($K > K_c$), the kinks are mobile, chain sliding is initiated by even the smallest driving force, and, accordingly, the static friction force vanishes, $F_s = 0$— the chain sliding is *superlubric*. On the other hand, below K_c the two incommensurate 1D surfaces are locked together due to pinning of the kinks that separate local regions of common periodicity, and in this case we expect stick-slip motion.

The kinetic friction properties of the FK model (Strunz and Elmer, 1998a, 1998b) are probed by adding a (e.g., Langevin) thermostat as described for the PT model above. Even where (above the Aubry transition) $F_s = 0$, the kinetic friction force F_k is nonzero, because the dynamics at any finite speed results in the excitation of phonons in the chain. Note also that a *finite-size $T = 0$ FK model* is always statically pinned, even for an irrational value of a_b/a_c because of the locking of the free ends of the chain. However an Aubry-like transition, exhibiting a symmetry-breaking nature, can still be defined (Braiman *et al.*, 1990; Benassi, Vanossi, and Tosatti, 2011; Pruttivarasin *et al.*, 2011). At finite T, pinning can be overcome by thermal fluctuations, which can initiate sliding even in the most-pinned state, the fully commensurate one; see Fig. 3. Finally, we remark that friction in the dynamically driven FK model describes fairly just the onset of sliding of a crystalline contact (Hammerberg *et al.*, 1998), while it cannot account for the highly inelastic plastic or quasiplastic deformations of the surfaces characterizing real-life friction experiments.

E. Superlubricity

Superlubricity is the phenomenon in which two incommensurate periodic surfaces may slide in dry contact with no atomic scale stick-slip instabilities which, as discussed above, are the main source for energy dissipation. Its physical origin is first that the energy of two interacting infinite incommensurate systems is independent of their relative position; and second that if they are hard enough, they will slide without stick-slip motion.

Vanishing static friction was first obtained within the FK model in the pioneering work of Peyrard and Aubry (1983) for mutually incommensurate periodicities, and sufficiently hard infinite lattices. Later, Hirano and Shinjo (1990, 1993) and Shinjo and Hirano (1993) predicted that for infinite incommensurate contacts the kinetic friction should also vanish, and they called this effect superlubricity. In these conditions, the lateral corrugation forces between two nonmatching, rigid crystals cancel out systematically, so that the kinetic friction of an externally driven solid vanishes at zero speed, and is dramatically reduced even at finite speed.

The term superlubricity has been criticized as misleading, since it might wrongly suggest zero friction in the sliding state in analogy to superconductivity and superfluidity. Instead, incommensurability of periodic interfaces cancels only one of the channels of energy dissipation, that originating from the low-speed stick-slip instability. Other dissipative processes, such as the emission of sound waves, still persist, and therefore even in the case of complete incommensurability the net kinetic friction force does not vanish. Nonetheless, in the superlubric regime one expects a substantial reduction of the friction force relative to a similar, but commensurate case.

Detailed experimental studies of superlubricity were recently performed by Dienwiebel *et al.* (2004, 2005) and Verhoeven, Dienwiebel, and Frenken (2004), who measured friction between a graphite flake attached to the FFM tip and an atomically flat graphite surface. Super-low friction forces (< 50 pN) are found for most relative orientations of the flake and the substrate, for which the contacting surfaces find themselves in incommensurate states (see Fig. 4). For narrow ranges of orientation angles corresponding to commensurate contacts, stick-slip motion was observed and friction was high (typically 250 pN). A few earlier experiments (Hirano *et al.*, 1991; Sheehan and Lieber, 1996) also provided indications of superlubricity in dry friction.

These observations of superlubricity can be described within a generalized PT model treating the graphite flake as
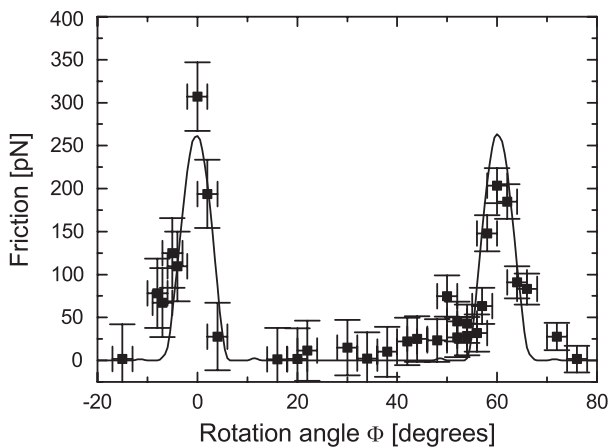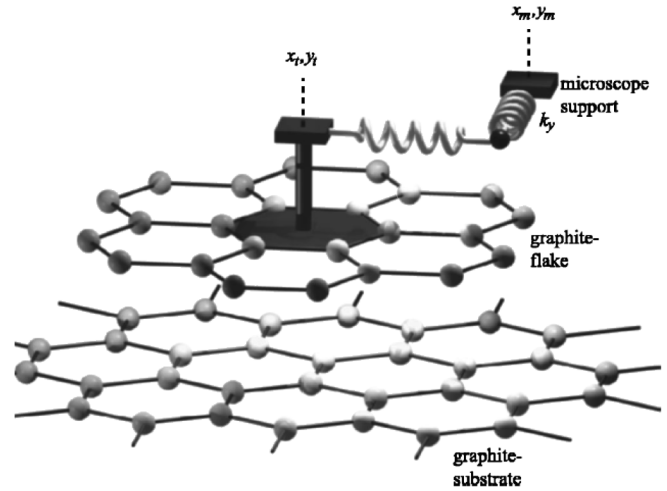

FIG. 5. The modified PT model used in the simulations of superlubricity. A rigid flake consisting of N atoms (here $N = 24$) is connected by an x spring and a y spring to the support of the microscope. The support is moved in the x direction. The substrate is modeled as an infinite rigid single layer of graphite. From Verhoeven, Dienwiebel, and Frenken, 2004.

a rigid finite lattice, composed of hexagonal carbon rings, as shown in Fig. 5. The interaction potential is obtained by summing the pairwise interactions between carbon atoms in the flake and in the graphite surface. The resulting flake-surface potential $U_{\text{flake}}(x_c, y_c, \phi)$ depends on the position of the center of mass of the rigid flake given by the two-dimensional coordinate $\mathbf{r}_c = (x_c, y_c)$, and on the orientational (misfit) angle ϕ of the flake relative to the surface lattice. The motion of the flake attached to the FFM tip and driven along the surface is described by the PT equation (2) where the sinusoidal tip-surface potential is replaced by the more complex potential $U_{\text{flake}}(x_c, y_c, \phi)$. Assuming that the flake is rotationally locked (i.e., ϕ is constant) the angular dependence of average friction force is in agreement with observations: The friction exhibits narrow peaks of high friction with stick-slip motion around the values of ϕ corresponding to the commensurate configurations of the flake and the surface, which are separated by wide angular intervals with smooth-sliding ultralow friction corresponding to incommensurate configurations (Verhoeven, Dienwiebel, and Frenken, 2004; Merkle and Marks, 2007). It should be noted that the angular width $\Delta\Phi$ of the friction maxima should depend on the flake size $\tan(\Delta\Phi) = 1/D$, where D is the flake diameter, expressed in lattice spacings. Accordingly, the width of friction peaks can be used to estimate the flake diameter.

Superlubricity between incommensurate surfaces provides a desired low-friction state essential for the function of small-scale machines. However, some experiments show that flake superlubricity has a finite lifetime: It disappears due to a reorientation of the flake into the commensurate state (Filippov *et al.*, 2008) as observed in a generalization of the PT model (Filippov *et al.*, 2008; de Wijn, Fusco, and Fasolino, 2010) and in tight-binding atomistic simulation (Bonelli *et al.*, 2009).

Studies of superlubricity may have important implications for understanding the macroscopic properties of graphite and other solid lamellar lubricants which are common solid

FIG. 4. The data points show the average friction force vs the rotation angle measured by Dienwiebel *et al.* (2004). The curve through the data points shows the calculated friction force from a generalized PT model for a symmetric 96-atom flake. From Verhoeven, Dienwiebel, and Frenken, 2004.

lubricants (Rapoport *et al.*, 1997; Singer, 1998; Heimberg *et al.*, 2001; Liu *et al.*, 2012). Mainly used as flaky powder, they are applied where liquid lubricants cannot be used, and show remarkable nanotribological properties which are still not understood. Recent MD simulations (de Wijn *et al.*, 2011) demonstrated that two surfaces lubricated by mobile, rotating graphene flakes may exhibit stable superlubric sliding as for ideally incommensurate contacts and for surfaces covered by randomly oriented pinned graphene patches. Under humid conditions, the multidomain surface structures can form spontaneously due to the capillary forces which fix randomly oriented flakes at the sliding surfaces, while in vacuum graphite patches are free to reorient to a high-friction and high-wear regime. This may provide an answer to the long-standing problem of why graphite is such a bad lubricant in vacuum, and needs the humidity of air to perform well (Savage, 1948).

F. Extensions of the Frenkel-Kontorova model

Many relevant generalizations of the FK model have been proposed so far to cover a large class of relevant frictional phenomena; they mainly consist of modifications of model interactions or of dimensionality. For realistic physical systems (as, e.g., atoms adsorbed on a crystal surface), anharmonicity can be introduced in the chain interatomic potential; see Braun and Kivshar (2004). The main novelties here include effects such as a broken kink-antikink symmetry, new types of dynamical solitons (supersonic waves), a breakup of the antikink soliton followed by a chain rupture, and a changed kink-kink interaction. Likewise, nonsinusoidal periodic substrates, characterized, e.g., by sharp bottoms and flat barriers (Peyrard and Remoissenet, 1982), have been investigated to address atoms adsorbed on simple metal surfaces. Complex unit cell substrates (Remoissenet and Peyrard, 1984; Vanossi *et al.*, 2003), as well as quasiperiodic (van Erp *et al.*, 1999; Vanossi *et al.*, 2000), and disordered corrugated profiles (Cule and Hwa, 1996; Guerra, Vanossi, and Ferrario, 2007) have also been considered in simulations. These deviations from the standard FK potential may lead to qualitatively different excitations such as different types of kinks, phonon branches, and changes in kink-antikink collisions. From a tribological point of view, different types of sliding behavior are to be expected at low-driving forces, when the dynamics is mainly governed by the motion of kinklike structures.

An important and more realistic generalization of the standard FK chain with relevant consequences for the resulting tribological properties (critical exponents, scaling of friction force with system size, mechanisms of depinning, etc.) involves increasing the dimensionality of the model. Especially the FK 2D generalized versions of the model (Persson, 2000a; Braun and Kivshar, 2004) are naturally applicable to the description of a contact of two solid surfaces (i.e., the case of "dry" friction), in particular, as is realized in QCM experiments, where 2D monatomic islands of adsorbate atoms slide over a periodic crystalline substrate (Krim and Widom, 1988). These approaches are especially powerful in the investigation of the transient behavior at the onset (or stopping) of sliding, which is quite difficult to study in fully realistic 3D models; see, e.g., Braun *et al.* (2001).

Noncontact AFM tips oscillating on top of kinklike adsorbate regions (Maier *et al.*, 2008) dissipate significantly more than near in-registry regions. This mechanism is explained by the higher softness and mobility of solitonic regions (Bennewitz *et al.*, 2000; Gauthier and Tsukada, 2000; Loppacher *et al.*, 2000; Hoffmann *et al.*, 2001), and it has been demonstrated by the dynamics of an incommensurate FK chain, forced and probed by a locally acting oscillation (Negri *et al.*, 2010).

In investigating confined systems under shear, FK-like models with just one particle (Rozman, Urbakh, and Klafter, 1996a, 1996b; Müser, 2002) or an interacting atomic chain (Rozman, Urbakh, and Klafter, 1997; Rozman, Urbakh, Klafter, and Elmer, 1998; Braun, Vanossi, and Tosatti, 2005) embedded between two competing substrates have led to uncovering of peculiar tribological phenomena related to stick-slip dynamics or to the appearance of "quantized" sliding regimes of motion (Santoro *et al.*, 2006; Vanossi *et al.*, 2006, 2007; Manini *et al.*, 2007; Castelli *et al.*, 2009). While some of these phenomena have been already observed, such as chaotic and inverted stick-slip motion, two types of smooth sliding and transitions between them (Drummond and Israelachvili, 2001; Drummond, Israelachvili, and Richetti, 2003), others are still waiting for experimental confirmation.

Last but not least, the combined Frenkel-Kontorova-Tomlinson (FKT) model (Weiss and Elmer, 1996, 1997) has been introduced including harmonic coupling of the interacting chain atoms to a sliding body. This approach resembles the Burridge-Knopoff model, detailed in Sec. IV.B, where, however, an on-site interaction with the lower body replaces a phenomenological dry friction law (usually a velocity-weakening one). The FKT model introduces more degrees of freedom than the PT model, and it has been used to describe effects of finite size and stiffness of the AFM tip and of normal load on friction (Igarashi, Nator, and Nakamura, 2008; Kim and Falk, 2009). The latter effect has been modeled assuming a linear dependence of the amplitude U_0 of potential corrugation on the applied normal force. The validity of the FKT model has been tested by 3D MD simulations (Kim and Falk, 2009), which confirmed the outcome of the model for most of investigated regimes except the limit of very low stiffness and high normal load. Unlike the FKT model, in which the breakdown of superlubricity coincides with the emergence of the metastable states, in the 3D model some metastable states appear to reduce frictional force leading to nonmonotonic dependence of force on normal load and tip compliance.

Increasing dimensionality and adding realistic features to the FK model brings its extensions into closer and closer contact to full-fledged MD simulations.

III. MOLECULAR-DYNAMICS SIMULATIONS

The simple low-dimensional MMs discussed in Sec. II are useful for a qualitative understanding of many physical aspects of friction. To address subtler features, such as the temperature dependence of the static friction of a specific interface or the Joule-heat dissipation, one should go beyond MMs including atomistic structural details of the interface. Such an approach is provided by MD simulations.

Advances in computing hardware and methodology have dramatically increased our ability to simulate frictional processes and gather detailed microscopic information for realistic tribological systems. MD simulations are used extensively in sliding nanofriction studies, to provide unique insight into the relevant processes, sometimes overturning conventional wisdom. They represent controlled computational experiments where the dynamics of all atoms is obtained by numerically solving Newtonian (or Langevin) equations of motion based on suitable interparticle interaction potentials and the corresponding interatomic forces. The geometry of the sliding interface and the boundary conditions (e.g., as sketched in Figs. 6 and 7) can be chosen to explore friction, adhesion, and wear. A thermostat, or other form of damping, is introduced in order to eliminate the Joule heat to obtain a frictional steady state. Finally, after specifying the initial coordinates and velocities of the particles, the classical differential equations of motion are integrated numerically.

A worthwhile guide to atomistic MD simulations of frictional processes focusing on fundamental technical aspects (realistic construction of the interface, appropriate ways to impose load, shear, and the control of temperature) can be found in the review articles by Robbins and Müser (2001) and by Müser (2006). For the general classical MD approach, we refer the interested reader to Allen and Tildesley (1991) and Frenkel and Smit (1996).

By following the Newtonian dynamics of a system executing sliding for a significant amount of time, quantities of physical interest such as instantaneous and average friction force, mean (center-of-mass) slider velocity, heat flow, and correlation functions are numerically evaluated. Unlike standard equilibrium MD simulations of bulk systems, frictional modeling inherently involves nonequilibrium conditions and a nonlinear dissipative response to the external driving. A standard practical assumption is to add Langevin terms to Newton's equations, as in Eqs. (2) and (3) for the PT model at finite temperature. We will return to this point later.

The choice of the appropriate interaction forces between atoms represents a major problem. If $U\{R_1, R_2, \ldots, R_N\}$ is the total energy of the system (here, say, the slider plus the substrate), as a parametric function of all atomic
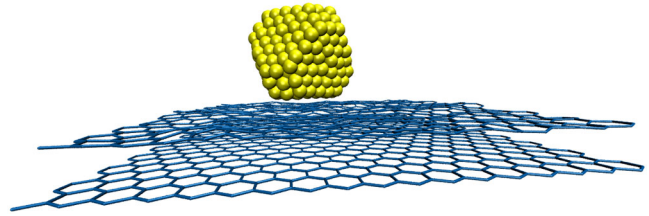
FIG. 7 (color online). A simulated truncated-octahedron Au_{459} cluster sliding with one of its (111) facets over a mobile graphite substrate. From Guerra *et al.*, 2010.

coordinates $\{R_i\}$, the force on atom i is $F_i = -\nabla_{R_i} U$, perfectly determined once U is known accurately. Unfortunately this is generally not the case, for U is determined by the quantum mechanics of electrons—a much bigger and unsavory problem to solve. *Ab initio* MD, e.g., of the Car-Parrinello type (Car and Parrinello, 1985), has not really been of use so far in sliding friction, mainly because it can handle only rather small systems, typically hundreds of atoms, for relatively short times, typically $\ll 1$ ns. Most MD frictional simulations are therefore based on reasonable empirical interatomic forces ("force fields"), ranging from relatively sophisticated energy surfaces accounting for electrons at the density-functional level or at the tight-binding level (Xu *et al.*, 1992), to angle-dependent many-particle potentials, to simple pairwise potentials (e.g., Lennard-Jones), to basic simple models of elastic springs, extensions of FK-type formulations. In practice, several reliable force fields, parametrized to fit different ranges of experimental data and material combinations, are available in the literature (Weiner *et al.*, 1986; Garrison and Srivastava, 1995; Brenner, Sherendova, and Areshkin, 1998; Ghiringhelli *et al.*, 2005; Los *et al.*, 2005). While this allows qualitative atomistic simulations of sliding friction, it is often far from quantitative. For example, during such a violent frictional process as wear, atoms may substantially change their coordination, their chemistry, and sometimes their charge. Once a specific system is understood after the elaborate development of satisfactory potentials, the mere change of a single atomic species may require a painful reparametrizationn of the interatomic forces. As a result, systematic frictional studies are a *tour de force* if no suitable set of consistent potentials is already available. A promising approach consists in the use of the so-called reactive potentials (Stuart, 2000; van Duin *et al.*, 2001; Brenner *et al.*, 2002), capable of describing chemical reactions and interface wear, with the advantage, for large-scale atomic simulations, of a good computational efficiency compared to first-principles and semiempirical approaches.

A. Thermostats and Joule heat

In a tribology experiment, mechanical energy is converted to Joule heat which is carried away by phonons (and electrons in metals). In a small-size simulation, the excitations generated at the sliding interface propagate and crowd into an excessively small region of "bulk" substrate, where they are backreflected by the cell boundaries, rather than properly dispersed away. To avoid overheating and in
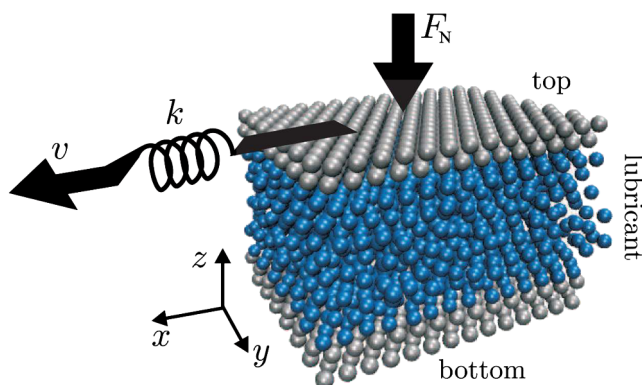

FIG. 6 (color online). Sketch of a typical MD simulation of a boundary-lubricated interface under shear. Periodic boundary conditions are applied in the x-y directions.

order to attain a frictional steady state, the Joule heat must therefore be steadily removed. If this removal is done by means of standard equilibrium thermostats such as velocity rescaling or Nosé-Hoover or even Langevin dynamics, an unphysical dissipation is distributed throughout the simulation cell, so that simulated atoms do not follow their real conservative motion, but rather execute an unrealistic damped dynamics which turns out to affect the overall tribological properties (Tomassone *et al.*, 1997). Similarly in the PT and FK models, the damping parameter γ is known to modify kinetic and frictional properties, but there is no clear way to chose the value of γ. To a lesser or larger extent, this lamentable state of affairs is common to all MD frictional simulations.

To solve this problem, one should attempt to modify the equations of motion inside a relatively small simulation cell so that they reproduce the frictional dynamics of a much larger system, once the remaining variables are integrated out. A recent implementation of a nonconservative dissipation scheme, based on early formulations by Magalinski (1959), and subsequent derivations by Li and E (2007), Kantorovich (2008), and Kantorovich and Rompotis (2008), has demonstrated the correct disposal of friction-generated phonons, even in the relatively violent stick-slip regime (Benassi *et al.*, 2010, 2012). All atoms near the sliding interface follow Newton equations, while the atoms in the deepest simulated layer, representing the boundary layer in contact with the semi-infinite heat bath (see Fig. 8), acquire additional nonconservative (and non-Markovian) terms which account for the time history of this layer through a memory kernel (Li and E, 2007; Kantorovich, 2008). Nanofriction simulations that exploit this dissipative scheme have recently been implemented, improving conceptually
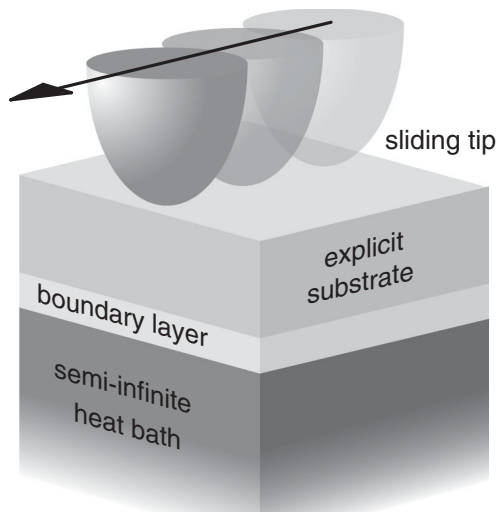

FIG. 8. Sketch of a MD simulation of friction. To account properly for heat dissipation, the infinitely thick substrate is divided into three regions: (i) a "live" slab comprising layers whose atomic motion is fully simulated by Newton's equations; (ii) a dissipative boundary zone, coincident with the deepest simulated layer, whose dynamics includes effective damping (e.g., non-Markovian Langevin-type) terms; and (iii) the remaining semi-infinite solid, acting as a heat bath, whose degrees of freedom are integrated out.

and practically over traditional Langevin simulations. Improvement is achieved, in particular, by adjusting the damping γ applied to the simulation boundary layer so as to variationally minimize the energy back-reflected by that boundary (Benassi *et al.*, 2012).

B. Size- and time-scale issues

Modern CPUs perform of the order of 10^9 floating-point operations per second (FLOPS) per core. Classical MD can take advantage of medium-scale parallelization, with fairly linear scaling to approximately 10^2 cores, thus affording about 10^{11} FLOPS. As the calculation of the force acting on each atom (usually the dominating step in a MD calculation) requires, depending on the complexity and range of the force field, about 10 to 10^2 FLOPS, the product of the number of simulated particles N times the number of time-integration steps N_{step} per runtime second on a modern medium-size parallel computer is given by $NN_{step} \simeq 10^{10}$. With a typical time step in the femtosecond range, a medium-size simulation involving $N = 10^5$ atoms can progress at a rate of 10^5 fs per second, i.e., approximately 10^9 fs $= 1$ μs in a simulation day. This total time scales down for larger systems sizes.

These estimates should be compared with the typical times, sizes, and speeds of tribology experiments. If we wish to address macroscopic sliding experiments, typical speeds would be in the 0.1 to 10 m/s range: In 1 μs the slider advances by 0.1 to 10 μm, i.e., approximately 10^3 to 10^4 typical lattice spacings, enough for a fair statistics of atomic-scale events (but hardly sufficient to gather significant data about phenomena such as the diffusion of additives or of wear particles within the lubricant, or step- or defect-related phenomena). In a nanoscale FFM experiment, however, the tip advances at a far smaller average speed (i.e., $\simeq 1$ μm/s) and we can simulate a miserable $\simeq 1$ pm advancement in a typical run, far too short to observe even a single atomic-scale event, let alone reaching a steady state. Therefore, whenever long-distance correlations and/or slow diffusive phenomena and/or long equilibration times are expected, MMs will perform better than fully atomistic MD simulations. There is nevertheless so much physical insight to be extracted from MD simulations that it makes sense to run them even at larger speeds than in AFM or SFA experiments; and indeed, the sliding speed adopted in most current atomistic MD frictional simulations is in the 0.1 to 10 m/s range.

One of the challenging problems for MD simulations is to account for the transition from stick-slip to steady sliding. In SFA and AFM experiments, stick slip with its associated hysteresis and large friction generally disappears for speeds larger than ~ 1 μm/s, while in MD simulations the transition takes place in the m/s range. This major discrepancy (up to ~ 6 orders of magnitude in speed) between simulations and experiments, has been discussed, e.g., by Braun and Röder (2002), Luan and Robbins (2004), and Braun and Naumovets (2006), and relates to the effective spring-force constants and mass distributions, that are largely different in the two cases, and much oversimplified in simulations. Several attempts to fill these gaps rely on methods, including hyperdynamics,

parallel-replica dynamics, temperature-accelerated dynamics, and on-the-fly kinetic Monte Carlo methods devised in recent years (Voter, Montalenti, and Germann, 2002; Mishin *et al.*, 2007; Kim and Falk, 2011).

Another important aspect present in experiments and largely missed by MD simulations is the aging of contacts due to the substrate relaxation. Aging can decrease substantially the critical velocity for the transition from stick-slip to steady sliding. Contact aging is also believed to be responsible for the increase of the static friction force as a function of the contact time. Direct imaging of contact regions in samples under a normal load show a logarithmic growth with time (Dieterich and Kilgore, 1994), leading therefore to increasing static friction. At the phenomenological level, frictional aging is well described by rate and state friction laws, widely used in geophysics (Ruina, 1983), but its microscopic origin is still debated. The main mechanisms that have been invoked in the past to explain it are plastic creep (Heslot *et al.*, 1994) or chemical strengthening at the interface (Li, Tullis *et al.*, 2011). In a recent paper, AFM was used to explore aging in nanoscale contact interfaces, finding supporting evidence for the second mechanism because, when the contact surface was passivated, it showed no more aging (Li, Tullis *et al.*, 2011). It is, however, likely that at larger scales and loads plastic creep would also play an important role. Beyond its direct relevance for friction, the intriguing issue of contact aging occurs in other non-equilibrium disordered systems such as granular media or glasses.

C. Multiscale models

Since it is currently impossible to treat atomistically all the characteristic length scales that mark the dynamical processes entering the friction coefficient of engineering materials, a rising effort is nowadays devoted to developing multiscale approaches. The basic consideration is that unless conditions are very special, all processes far away from the sliding interface can be described at least approximately by continuum mechanics, and simulated using finite elements, allowing for a macroscopic description of elastic and plastic deformation. The advantage of these continuum-theory methods is that it is possible to increasingly coarse grain the system as one moves away from the sliding contact, thereby highly reducing the computational effort. Several groups (Luan *et al.*, 2006; McGee and Smith, 2007) combine the atomistic treatment of the interfacial mating region, where displacements occur on an atomic or larger length scale, with a coarse-grained or finite-element continuum description elsewhere, where strains are small and continuous. The main difficulty lies in the appropriate matching conditions between the atomistic and continuum regions (E, Ren, and Vanden-Eijnden, 2009). Since the atomic detail of lattice vibrations (the phonons), which are an intrinsic part of the atomistic model, cannot be fully represented at the continuum level, conditions must be met, for example, that at least the acoustic phonons should not be excessively reflected at the atomistic-continuum interface. In other words, matching at this interface must be such that long wavelength deformations should transmit with reasonable accuracy in both directions,

which is vital to a proper account of Joule-heat disposal into the bulk.

D. Selected applications of MD in nanotribology

We survey here some recent results from the growing simulation literature, mostly from our groups, and certainly not providing an adequate review of the field.

1. Boundary lubrication in confined systems

Hydrodynamics and elastohydrodynamics have been very successful in describing lubrication by microscopically thin films. With two sliding surfaces well separated by a hydrodynamically fluid film, friction is mainly determined by the lubricant viscosity. The friction coefficient can be calculated using the Navier-Stokes equations, showing a monotonic increase with the relative sliding velocity between the two surfaces (Szeri, 2001). For small driving velocity and/or high load, the lubricant cannot usually keep the surfaces apart and solid-solid contact eventually ensues. Even before full squeezout, a liquid confined within a nanometer-scale gap ceases to behave as a structureless fluid. Pioneering studies of confined systems under shear reveal a sequence of drastic changes in the static and dynamic properties of fluid films in this "boundary-lubrication" regime.

SFA experiments (Yosbizawa and Israelachvili, 1993) and MD simulations (Gao, Luedtke, and Landman, 1997a, 1997b) have both shown clear upward frictional jumps, in correspondence to squeezeout transitions from N to $N-1$ lubricant layers. The lubricant squeezeout for increasing load becomes harder and harder, corresponding to a (near) crystallization of the initially fluid lubricant (Persson and Tosatti, 1994; Persson and Mugele, 2004; Tartaglino *et al.*, 2006). Owing to layer-by-layer squeezeout, there will be frictional jumps for increasing load. Friction would not necessarily always jump upward, because restructuring of the solidified trapped lubricant film, and/or a switching of the maximum shear gradient from within the lubricant layer (possibly accompanied by local melting), to the lubricant-slider interface may take place. It could jump downward, in particular, if lattice mismatch between the compressed boundary lubricant layer and the rigid substrates jumped, say, from commensurate to incommensurate, the latter superlubric with a mobile soliton pattern, as sketched in Fig. 9. Possibilities of this kind have been the object of recent investigation (Vanossi *et al.*, 2013).

Simulations also show that the presence of impurities or defects between two incommensurate stiff sliding surfaces can, even in a relatively small concentration, lead to pinning and nonzero static friction (Müser and Robbins, 2000). Defects can destroy superlubricity by introducing mechanical instabilities, which may occur depending on the system dimensionality, the structure and relative orientation of the confining walls, and the detail of the lubricant-wall interactions.

MD investigations of a melting-freezing mechanism in the stick-slip phenomenology of boundary-lubricated films were carried out by Thompson and Robbins (1990) and Stevens and Robbins (1993). Various realistic models for lubrication layers in very specific contexts have been investigated with extensive MD simulations (Chandross *et al.*, 2004, 2008;
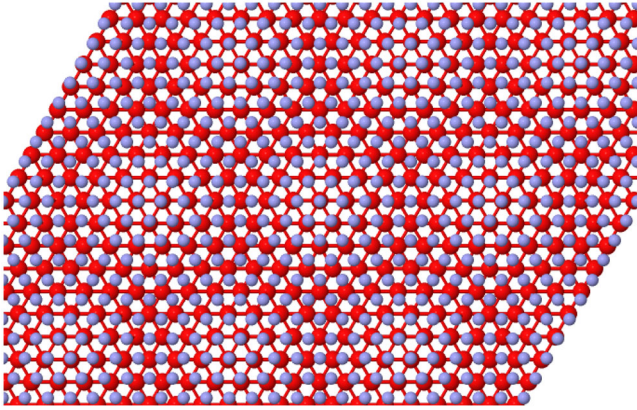
FIG. 9 (color online).   A snapshot of a MD simulation of the 2D solitonic pattern in the boundary layer of a solid lubricant (clear) in contact with a perfect crystalline surface (dark), induced by a 16% lattice-constant mismatch. The Lennard-Jones interaction of this simulation favors in-registry hollow sites, while unstable top sites mark solitonic regions. Other layers were omitted for clarity.

Braun and Naumovets, 2006; Lorenz, Chandross, and Grest, 2010; Lorenz, Chandross, Lane, and Grest *et al.*, 2010).

2. Sliding of absorbed monolayers

An ideal experimental setup to investigate the molecular origin of friction is provided by the QCM, where atomically thin systems, usually just one monolayer or less of rare gas is deposited on a substrate resting on a quartz crystal. When the crystal surface oscillates strongly enough so as to dislodge the adsorbate islands under their own inertial force, the sliding friction is revealed by mechanical damping. Depending on the substrates and on the system interactions at play, the equilibrium properties of these systems may exhibit distinct structural geometries, of interest in the field of 2D phase transitions; different dynamical phases may show up for the driven over layer, such as pinned solid, sliding solid, and liquid phases (Krim, Solina, and Chiarello, 1991; Bruschi, Carlin, and Mistura, 2002; Krim, 2007).

These experimentally well-characterized systems have also been studied theoretically and numerically by molecular dynamics simulations (Cieplak, Smith, and Robbins, 1994; Persson and Nitzan, 1996; Sokoloff and Tomassone, 1998; Braun *et al.*, 2001; Granato and Ying, 2004). When the interface is commensurate, the static friction is too large to allow for a massive slip (Cieplak, Smith, and Robbins, 1994); yet slip is observed experimentally for a Xe monolayer on a Cu(111) substrate, a system that forms a commensurate interface (Coffey and Krim, 2005). A possible explanation is a slip which does not occur coherently but by a nucleation process in which a bubble slips forward creating a new commensurate domain as revealed by MD simulations (Reguzzoni *et al.*, 2010). It is possible to estimate the critical radius of this domain and the energy barrier associated with the nucleation process by the conventional theory of nucleation, estimating the value of the relevant parameters from a solution of an effective FK model (Braun and Kivshar, 2004). Thanks to thermally activated nucleation, with the additional help of impurities and disorder acting as seeds, the monolayer can slip under lateral forces that are much smaller than those

expected for a rigid layer pinned by the commensurate interface, providing an explanation for the experimental results.

When the adsorbate is incommensurate and hard, solitons exist already in the ground state, and their free motion should in principle permit superlubric sliding. If, however, the adsorbate forms islands, as should generally be the case, perfect superlubricity is still broken by the island's edges, which present a barrier to the entering and exiting of solitons, necessary for the island to slide. This island edge pinning is currently the object of ongoing studies.

3. Extreme temperature and speed conditions

An advantage of MD is that it can address extreme or otherwise unusual frictional situations, still unexplored because they may be experimentally difficult to realize. One such example are the high "flash temperature" regimes caused by local Joule heating due to wear and other machining or braking conditions (Bowden and Tabor, 1950). Even in equilibrium but at temperatures close to the melting point, the outermost layers of a solid substrate generally undergo "surface melting" (Tartaglino *et al.*, 2005). In these conditions, AFM nanofriction cannot generally be experimentally accessed, because the nearly liquefied surface layers jump to contact and wet the tip long before it reaches nominal contact (Kuipers and Frenken, 1993). However, some solid surfaces, such as NaCl(100), do not melt (Zykova-Timan *et al.*, 2005), thus making for an interesting, albeit purely theoretical so far, case study. MD simulations predict that high-temperature nanofriction over such a nonmelting surface would behave very differently depending whether the tip-surface contact is "hard" or "gentle." In the first case, the tip plows the substrate with wear. The friction coefficient, very large at low temperature, drops close to the melting point, when the tip itself provokes local melting, and moves accompanied by its own tiny liquid droplet, precisely as in ice skating. For gentle, low-load, wear-free sliding on a hard surface, the opposite is predicted. Here friction, initially very small, is expected to increase as temperature is raised close to the melting point where the surface, still solid, becomes softer and softer due to increasing anharmonicity, with an analogy to flux lines in type II superconductors (Zykova-Timan, Ceresoli, and Tosatti, 2007).

A second example is high-speed nanofriction, as could be expected by a tip or a surface-deposited nanocluster (see Fig. 7) sliding at large speed over a smooth crystal surface. A speed in excess of 1 m/s is many orders of magnitude higher than that of ordinary AFMs or other nanofrictional systems, and is as yet unexplored. MD simulations, carried out for the test case of gold clusters sliding over graphite surfaces, show, besides a standard low-speed drift sliding regime, the emergence of a novel "ballistic" sliding regime, typically above 10 m/s (Guerra *et al.*, 2010). The temperature dependence of the cluster slip distance and time, measuring its sliding friction, is predicted to be opposite in these two regimes, high-speed ballistic sliding and low-speed drift sliding. The interplay of rotations and translations is crucial to both regimes. Simulations show that the two are correlated in slow drift but anticorrelated in fast ballistic sliding. Despite the large difference with drift, the speed dependence of ballistic friction is, as with drift, viscous, a

useful result whose validity was not discounted in principle, and which it would be interesting to pursue and test experimentally.

4. Nanomanipulation: Pinning versus diffusion

AFM manipulation of surface-deposited clusters can serve as a useful method to measure the interfacial friction of structurally well-defined contacts of arbitrary size and material combinations. Here MD simulations are extremely useful in understanding depinning, diffusion, and frictional mechanisms of clusters on surfaces. Indeed, one of the remarkable experimental observations of the last decade concerns the unexpected ability of relatively large metal clusters to execute friction-free motions and even long jumps with size and shape conservation (Bardotti *et al.*, 1996; Dietzel *et al.*, 2008; Paolicelli *et al.*, 2008, 2009; Brndiar *et al.*, 2011). Gold clusters, comprising typically hundreds of atoms, have been repeatedly observed to diffuse on highly oriented pyrolytic graphite (HOPG) surfaces with surprisingly large thermally activated diffusion coefficients already at room temperature; a similar behavior was reported also for larger antimony clusters. MD simulations of the diffusive regime have shown the possible coexistence of sticking periods, and of long jumps, reminiscent of so-called Lévy flights (Luedtke and Landman, 1999; Lewis *et al.*, 2000; Maruyama, 2004; Guerra *et al.*, 2010). The sticking lasts so long as the cluster-substrate surfaces are orientationally aligned, and the long sliding jumps occur when a thermal fluctuation rotates the cluster destroying the alignment (Guerra *et al.*, 2010). Further understanding of the sliding of these deposited nano-objects will be of considerable future value (Schirmeisen and Schwarz, 2009).

5. Simulated frictional control

Exploring novel routes to achieve friction control by external physical means is an important goal currently pursued in nanotribology. Two methods have recently been suggested by simulation: mechanical oscillations and phase transitions.

Mechanical oscillations.—Natural or artificially induced oscillations obtained by small normal or lateral mechanical vibrations may, when applied at suitable frequency and amplitude ranges, help drive a contacting interface out of its potential-energy minima, considerably increasing surface mobility and diffusion, and reducing friction and wear. Flexibility and accessibility are the main relevant features of this approach, since frictional properties can be tuned continuously by the frequency and the amplitude of the applied vibrations. This effect has been demonstrated experimentally with AFM (Riedo *et al.*, 2003; Jeon, Thundat, and Braiman, 2006; Socoliuc *et al.*, 2006; Lantz, Wiesmann, and Gotsmann, 2009) (see Fig. 10), and in sheared confined system (Heuberger, Drummond, and Israelachvili, 1998; Bureau, Baumberger, and Caroli, 2000; Cochard, Bureau, and Baumberger, 2003), and numerically with atomistic MD (Gao, Luedtke, and Landman, 1998; Capozza *et al.*, 2009; Capozza *et al.*, 2012) or MM approaches (Rozman, Urbakh, and Klafter, 1998; Zaloj, Urbakh, and Klafter, 1999; Tshiprut, Filippov, and Urbakh, 2005). On a larger scale, it has also been reported that in sheared granular media experiments the stick-slip behavior is also significantly perturbed by small transverse vibrations (Johnson and Jia, 2005; Johnson *et al.*, 2008; Capozza *et al.*, 2011; Krim, Yu, and Behringer, 2011). Despite these promising numerical and experimental contributions, a detailed analysis accounting for the friction dependence on vibrations is still to some extent lacking. Most past theoretical studies of mechanical control adopted an oversimplified single-asperity model, which misses the collective behavior of multiasperity mesoscopic interfaces. This and other aspects of interface oscillation are still calling for a proper treatment and understanding.

Phase transitions.—Another idea to control friction is to employ a substrate undergoing a phase transition. While it is obvious that friction will change in the presence of a phase transition, it is more subtle to precisely qualify and quantify the effect. Surprisingly perhaps for such a basic concept, there are essentially no experimental data available—and no theory either. While it would be tempting to use linear-response theory (Ala-Nissila, Han, and Ying, 1992), with the fluctuation-dissipation theorem making direct contact between criticality and viscous friction, one cannot ignore that realistic dry friction is dominated by stick-slip instabilities that are intrinsically violent and nonlinear. Hence, one is left with MD simulations. A PT-like MD nanofrictional simulation based on a point slider over a 2D model substrate with a built-in structural displacive transition recently predicted that stick-slip friction should actually peak near the substrate critical temperature (Benassi, Vanossi,
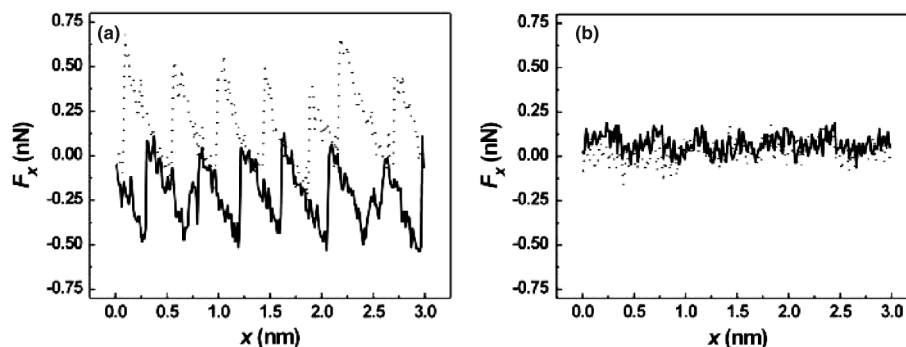
FIG. 10.   The effect of oscillations on the lateral force detected by AFM scanning forward (solid curve) and backward (dotted curve) on an atomically flat NaCl surface. An average normal load $F_N = 2.73$ nN was kept constant (a) without a bias voltage between the cantilever and the sample holder, and (b) with an applied ac voltage with frequency $f = 56.7$ kHz and amplitude 1.5 V. From Socoliuc *et al.*, 2006.

Santoro, and Tosatti, 2011). These results show that friction will also depend upon the order parameter direction, a dependence due to the different ability of the slider to elicit disorder in the substrate depending on that direction. Some level of control of atomic-scale friction can thus be anticipated through external switching of the order parameter direction (e.g., by an external field or strain). Although the magnitude of the phase transition effects relative to the background friction will of course depend on the real system chosen, these results suggest pursuing this idea experimentally in, e.g., displacive ferrodistortive and antiferrodistortive materials, a vast realm of solids exhibiting continuous or nearly continuous structural transitions.

IV. MULTICONTACT MODELS

The PT model discussed in earlier sections provides a good initial description of the frictional behavior of an individual contact that can be relevant for nanotribology experiments. However, recent simulations (Mo, Turner, and Szlufarska, 2009) revealed that, even for an apparently sharp AFM tip sliding on a crystalline surface, the actual interface consists of an ensemble of individual atomic contacts (see Fig. 11). On larger scales such as the mesoscale of SFA experiments, the multicontact picture becomes even more obvious. The way individual contacts can be averaged to yield macroscopic friction law has been the focus of intense research in recent decades. Friction is not simply the sum of single-asperity responses, but is influenced by temporal and spatial dynamics across the entire ensemble of contacts that form the frictional interface. Long-range elastic interactions between contacts are important and cannot be neglected. Persson (2001) and Persson *et al.* (2005) greatly improved and generalized these concepts to more realistically fractal rough surfaces.
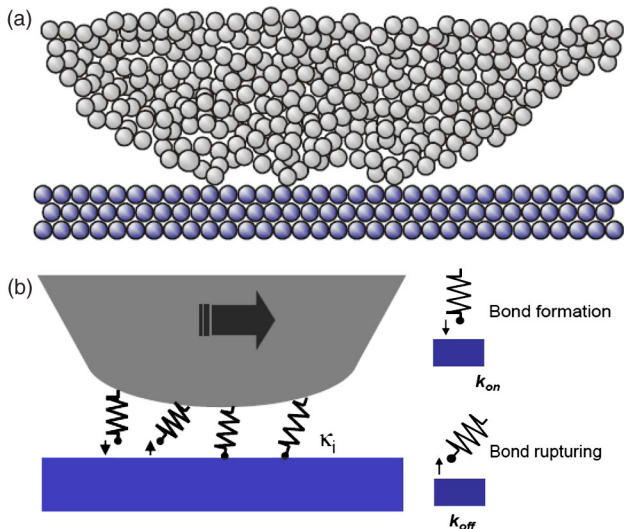

FIG. 11 (color online). Multicontact modeling. (a) Sketch of a typical geometry for an amorphous tip sliding on a flat crystalline surface. (b) A model to simulate multiple contacts at the tip-sample interface. Rates of contact formation and rupturing processes are determined by the heights of the corresponding energy barriers, ΔE_{on} and ΔE_{off}. Adapted from Barel *et al.*, 2010a.

A. Mechanokinetic models

Significant progress in the solution of these problems was recently achieved with coarse-grained mechanokinetic models (Persson, 1995; Braun and Röder, 2002; Filippov, Klafter, and Urbakh, 2004; Braun, Barel, and Urbakh, 2009; Barel *et al.*, 2010a, 2010b) that describe friction through dynamical rupture and formation of interfacial contacts (junctions). These contacts may represent molecular bonds, capillary bridges, asperities between rough surfaces, and for lubricated friction they can mimic patches of solidified lubricant or its domains. Each contact is modeled as an elastic spring connecting the slider and the underlying surface. As long as a contact is intact (unbroken), it is increasingly stretched with a speed equaling the velocity of the slider, and thus produces an increasing force that inhibits the motion; after the instability point is reached, a ruptured contact relaxes rapidly to its unstretched equilibrium state. The kinetics of contact formation and rupturing processes depends on the physical nature of contacts. For atomic-scale contacts, capillary bridges and domains of solidified lubricants, the processes of rupture and formation of contacts are thermally activated, and the interplay between them may lead to a complex dependence of friction on slider velocity and sample temperature (Persson, 1995; Braun and Röder, 2002; Filippov, Klafter, and Urbakh, 2004; Braun, Barel, and Urbakh, 2009; Braun and Tosatti, 2009; Barel *et al.*, 2010a, 2010b; Barel *et al.*, 2012). For microscopic and macroscopic asperities between rough surfaces, thermal effects are less significant and threshold rupture forces should be taken from a distribution that is determined by the structure of the contacting surfaces. The mechanism of contact detachment is similar to the one proposed previously by the fiber-bundle models (Alava, Nukala, and Zapperi, 2006).

At the nanoscale, the rates of formation k_{on} and rupturing k_{off} of microscopic contacts are defined by the corresponding energy barriers ΔE_{on} and ΔE_{off}. The barrier for detachment ΔE_{off} is force dependent and diminishes as the force acting on the contact increases and the contact is stretched. As discussed above, precisely this mechanism characterizes the PT model, but what has rarely been rationalized so far is that the process of contact formation must be considered as well.

The dynamics of friction in the mechanokinetic models is determined by four characteristic rates: (i) the rate k_{off}^0 of spontaneous detachment of contacts, (ii) the rate k_{on} of contact formation, (iii) the rate Kv/f_s of forced unbinding, and (iv) a characteristic rate of the pulling force relaxation, $\omega_m = \max(K/\gamma m, \sqrt{K/m})$. Here f_s is an average threshold force for the contact rupture, K is the stiffness of the pulling spring, γ is the dissipation constant, and m is the mass of the slider. Correspondingly, these models exhibit three regimes of motion: (i) smooth sliding at very low velocities or high temperatures, with $k_{off}^0 > Kv/f_s$; (ii) smooth sliding also for high velocities or low temperatures, with $k_{on} < Kv/f_s$; and (iii) stick-slip oscillations for intermediate velocities and temperatures. These multicontact models demonstrate that the overall smooth sliding corresponds to uncorrelated atomic-scale stick-slip (or smooth) motion of individual junctions, while the global stick-slip motion emerges from a cooperative behavior of the junction subsystems. It is

interesting to note that the transition from smooth sliding to stick slip with increasing v was indeed observed in SFA experiments with two weakly adhering boundary-lubricated surfaces (Drummond, Israelachvili, and Richetti, 2003).

An important advantage of the mechanokinetic models is that they are directly scalable to mesoscales and macroscales. Application of these models has already allowed the resolution of some significant disagreements between the experimental observations and the predictions of the PT model and MD simulations. First, SFA experiments found that the critical velocity for transition from stick-slip motion is in the interval of 1–10 μm/s, while the MD simulations and PT model lead to values which are 6 or 7 orders of magnitude larger (Braun and Röder, 2002; Luan and Robbins, 2004; Braun and Naumovets, 2006). According to the mechanokinetic models, the transition should occur at $v \approx f_s k_{on}/K$ that for reasonable values of the parameters agrees with the experimentally observed values of the critical velocity. Second, the PT model and MD simulations (Brukman *et al.*, 2008; Steiner *et al.*, 2009; Dong *et al.*, 2011) fail to reproduce the nonmonotonic temperature dependence of the average friction force found in FFM experiments for several material classes. The mechanokinetic model demonstrates that the peak in the temperature dependence of friction emerges from two competing processes acting at the interface: the thermally activated formation and rupturing of an ensemble of atomic contacts (Barel *et al.*, 2010a, 2010b, 2011). This observation also provides a direct link between the temperature and velocity dependencies of friction and it shows the experimentally observed fingerprint in the friction-velocity curves. Specifically, at temperatures above the peak temperature, friction increases with scan speed, whereas, below the peak, friction decreases with velocity.

An important and still unresolved question is what is the microscopic origin of the rupture and reattachment processes introduced for the interpretation of FFM experiments (Filippov, Klafter, and Urbakh, 2004; Barel *et al.*, 2010a, 2010b). Similarly to the mechanism of energy dissipation in AFM (Kantorovich and Trevethan, 2004; Ghasemi *et al.*, 2008), they can be attributed to reversible jumps of surface atoms, flips of surface fragments, or transitions between different tip structures, which are induced by the tip motion along the surface. These dissipative processes result in a bistable potential-energy profile for the tip-surface junction where the barrier separating the potential minima is continuously changed during sliding. An unambiguous understanding of the nature of the corresponding instabilities and evaluation of microscopic parameters which determine the values of the rupture and reattachment rates require first-principles calculations of potential-energy surfaces for the tip-surface junctions. The first attempts in bridging the gap between mechanokinetic models and MD simulations have already demonstrated that model parameters can be completely specified using information obtained from fully atomistic simulations (Perez *et al.*, 2010; Liu and Szlufarska, 2012). Then the parameter-free kinetic models are able to reproduce the temperature and velocity variation in the friction force as obtained from fully dynamical atomistic simulations with very high accuracy over a wide range of

conditions. This combined approach is promising because it allows the full atomistic details provided in MD simulations to be used in interpreting experimental phenomena at time and length scales relevant to tribological measurements.

B. Elastic interactions and collective effects

Elastic instabilities play, as we saw, a prominent role in explaining frictional dissipation at the nanoscale and one may thus ask what happens at larger scales for multicontact interfaces. The role of elasticity in friction crucially depends on whether stress gradients are present or not (Lorenz and Persson, 2012). For uniform loading, stress is distributed homogeneously on the contact surface and elastic interactions mediate the response of local slip fluctuations. Experimental conditions, however, often lead to shear stress concentration at the edge of the sample leading to detachment fronts. We discuss the first case in this section and the second case in Sec. IV.C.

The interplay between small-scale disorder due to random contacts and elastic interactions between the contacts is a complex statistical mechanics problem that is encountered in different contexts from vortex lines in superconductors (Larkin and Ovchinnikov, 1979), dislocations in solids (Labusch, 1970), and domain walls in ferromagnets (Hilzinger and Kronmüller, 1976) to name just a few. Two bodies in contact form a set of n random contacts per unit area. In the limit of small uniform loads, we can consider a weak-pinning hypothesis, in which friction results from the fluctuations of the forces due to individual contacts, and derive a scaling theory (Volmer and Nattermann, 1997; Caroli and Nozières, 1998; Persson and Tosatti, 1999; Sokoloff, 2002a; Bruan *et al.*). Neglecting for simplicity tensor indices, the displacement of a contact at **x** due to the elastic interactions with the other contacts can be estimated as

$$u = \int d^2 x' G(\mathbf{x} - \mathbf{x}')\sigma(\mathbf{x}'), \tag{7}$$

where the elastic Green's function scales as $G(\mathbf{x}) \sim 1/(E|\mathbf{x}|)$, E is the Young modulus (which is typically 10–100 times larger than the yield strength σ_Y), and the contact stresses σ are randomly distributed with zero mean correlations,

$$\langle \sigma(\mathbf{x})\sigma(\mathbf{x}') \rangle = n\sigma_Y^2 a^4 \delta(\mathbf{x} - \mathbf{x}'), \tag{8}$$

where a is the contact diameter, depending on the normal load, the yield stress σ_Y is taken as a measure of the stress due to the contacts, and n is the contact density. In analogy with other collective pinning theories, we can estimate the typical length scale L_c [usually referred to as the "Larkin length" (Larkin and Ovchinnikov, 1979) or "elastic coherence length" (Persson and Tosatti, 1999; Müser, 2004)] at which elastic interaction becomes important by the condition that the typical displacement equals the size of the contact $\langle u^2 \rangle = a^2$. A straightforward calculation yields

$$L_c = a \exp\left(C \frac{Ed}{\sigma_Y a} \right)^2, \tag{9}$$

where C is a numerical constant and $d = 1/\sqrt{n}$ is the average distance between contacts. The Larkin length separates the length scales for which elastic interaction dominates

($L < L_c$) and the contact interface does not deform from those at which disorder dominates ($L > L_c$) and interface adapts to the pinning-center landscape. For two macroscopic bodies in contact, Eq. (9) predicts that L_c is very large because $d \gg a$ and $E \gg \sigma_Y$, and pinning-induced deformations should be absent. One should bear in mind that a boundary-induced stress gradient can still lead to observable elastic deformations, as discussed in Sec. IV.C.

An important aspect that is missing from the analysis above is the presence of long-range correlations: Most contact surfaces are self-affine over several length scales. This implies that the assumption of uncorrelated surface stresses made in Eq. (8) is not valid. One can, however, repeat the Larkin argument for long-range correlated pinning stresses,

$$\langle \sigma(\mathbf{x})\sigma(\mathbf{x}') \rangle = \sigma_Y^2 \left(\frac{a}{|\mathbf{x} - \mathbf{x}'|} \right)^\gamma, \qquad (10)$$

where γ is a scaling exponent. Computing the typical displacement in this case, we obtain

$$L_c \propto a \left(\frac{E}{\sigma_Y} \right)^{2/(2-\gamma)} \qquad (11)$$

for $\gamma < 2$, while for $\gamma \geq 2$ long-range correlations are irrelevant (Fedorenko, Doussal, and Wiese, 2006) and we recover the uncorrelated case in Eq. (9). The interesting feature of Eq. (11) is that the dependence is not exponential and the contact interface can deform even at small length scales. The effect of elastic interactions due to the contact of self-affine surfaces has been studied analytically and numerically, revealing that the solid indeed deforms elastically due to the contact (Persson, 2006; Campana, Müser, and Robbins, 2008; Campana, Persson, and Müser, 2011).

The role of elasticity in friction is vividly illustrated by the Burridge-Knopoff model for earthquakes (Burridge and Knopoff, 1967; Carlson, Langer, and Shaw, 1994) where a set of frictional blocks of mass M coupled by springs are driven over a substrate (see Fig. 12). In one dimension, the equation of motion for the displacement u_i of block i is given by

$$M\ddot{u}_i = K_0(u_{i+1} + u_{i-1} - 2u_i) + K_d(u_i - ia - vt) + f(\dot{u}_i), \qquad (12)$$

where K_0 and K_d are the stiffnesses of the springs connecting the blocks between themselves and with the loading plate that moves at constant velocity v. Here $f(v)$ is a phenomenological friction force that decreases with the velocity of the block and a is the rest length of the springs connecting the blocks.

The Burridge-Knopoff model is a deterministic model but displays a very rich dynamical behavior with widely distributed slip events. The key to the instability is the velocity-weakening constitutive law $f(v)$ employed to describe the frictional properties of each block. The model thus operates at
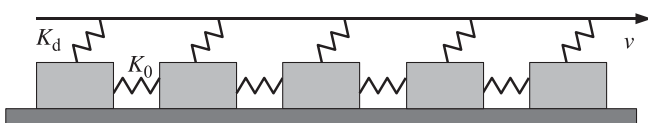

FIG. 12. A sketch of the Burridge-Knopoff model. A set of frictional blocks connected by springs of stiffness K_0 are attached to a slider moving at velocity v by a set of springs of stiffness K_d.

a macroscopic scale and one needs to justify microscopically the origin of its constitutive law. In this context the model serves to illustrate the concept of localized instabilities during friction: On the tectonic scale, slip is localized on some portion of the fault that does not necessarily move coherently as a rigid block.

C. Mesoscale friction: Detachment fronts

Significant progress in understanding the relationship between the dynamics of individual contacts and macroscopic frictional motion has been achieved with the development of a new real-time visualization method of the net area of contact along the entire interface, as discussed in a series of papers by Fineberg's group (Rubinstein, Cohen, and Fineberg, 2004, 2006, 2007; Ben-David, Cohen, and Fineberg, 2010; Ben-David and Fineberg, 2011). In their experimental apparatus, two poly(methyl methacrylate) (PMMA) blocks were pressed together and sheared by a constant force. A similar visualization technique has been used for tribological studies of a different transparent material, Columbia resin (Nielsen, Taddeucci, and Vinciguerra, 2010). Owing to the transparency of the media, it was possible to record the contact area as the blocks were slipping. This method has enabled a number of key conclusions to be drawn on the mechanism of transition from static to kinetic friction in macroscopic systems: (i) the onset of sliding is preceded by a discrete sequence of cracklike precursors (collective modes of the entire ensemble of asperities); (ii) the transition is governed by the interplay between three types of fronts: sub-Rayleigh, intersonic, and slow fronts; and (iii) a sequence of precursor events gives rise to a highly inhomogeneous spatial distribution of contacts before the overall sliding occurs. The collective behavior of the asperity ensemble that composes a frictional interface therefore determines the transition mechanism from static to kinetic friction. Imaging the contacts during friction also allowed recording of the local values of shear and normal stresses. By doing this, Ben-David and Fineberg (2010) showed that the friction coefficient is not a constant material property but it also depends on the way the system is loaded locally (Ben-David and Fineberg, 2011). These results call into question many assumptions that have ruled studies of friction for centuries: If the onset of sliding occurs by the propagation of fronts then elastic deformations in the contact interface become relevant and should be taken into account by a theory of friction. This may even challenge the Amontons law stating that the friction coefficient is independent on the normal load and on the apparent contact area. Indeed deviations from Amontons' laws have been reported for this experiment.

The experimental phenomenology is well captured by a minimal spring-block model (Braun, Barel, and Urbakh, 2009; Capozza and Urbakh, 2012) that describes friction at the slider-substrate interfaces in terms of rupture and reattachment of surface junctions, which represent asperities between rough surfaces. Contrary to the above discussed Burridge-Knopoff model of earthquakes where phenomenological friction laws have been introduced, the model of Braun, Barel, and Urbakh (2009) explicitly includes two

most relevant material properties: interfacial elasticity and thresholds for yielding or rupture of surface junctions. The interfacial elasticity, which was ignored in previous commonly used models of friction, defines a new velocity scale that is independent of the Rayleigh speed and corresponds to slow cracklike fronts (Rubinstein, Cohen, and Fineberg, 2004, 2006; Nielsen, Taddeucci, and Vinciguerra, 2010) mediating the transition from static to kinetic friction.

The spring-block model (Braun, Barel, and Urbakh, 2009) motivated a continuum description of friction between spatially extended materials that includes a coupling between the bulk elastic deformations and the dissipative dynamics at frictional interfaces, which mimic the rupture and reattachment of microcontacts (Bouchbinder *et al.*, 2011; Bar Sinai, Brener, and Bouchbinder, 2012). This promising approach may bridge a gap between microscopic and macroscopic scales and enable simulations of macroscopic friction processes at time and length scales relevant to tribological measurements.

The 1D spring-block models discussed above (Burridge and Knopoff, 1967; Carlson, Langer, and Shaw, 1994; Braun, Barel, and Urbakh, 2009) have limitations, which do not allow a quantitative description of macroscopic friction experiments. In particular, the 1D models predict an exponential decay of elastic interactions within the sample, while a 3D description leads to a power-law decrease of the stress. Nevertheless, recent 2D calculations employing a spring-block model (Trømborg *et al.*, 2011) and finite-element method (Kammer *et al.*, 2012) demonstrated that the 1D models provide an important insight into the mechanism of dry friction between spatially extended materials, and allow one to investigate the effect of system parameters on frictional response. It is important to note that, in order to reproduce experimentally the observed spectrum of detachment fronts, the models should incorporate interfacial stiffness and local friction laws including both velocity weakening and strengthening branches (Braun, Barel, and Urbakh, 2009; Bouchbinder *et al.*, 2011; Bar Sinai, Brener, and Bouchbinder, 2012). The models assuming local Coulomb-Amontons friction at the block-substrate interface (Trømborg *et al.*, 2011) do not exhibit slow rupture fronts like those observed in various experiments (Rubinstein, Cohen, and Fineberg, 2004, 2006; Nielsen, Taddeucci, and Vinciguerra, 2010). A quantitative comparison to experimental data requires 2D calculations with a proper choice of local friction laws that is a challenge for future studies.

Several questions still remain open: How general are these experimental results? Do they depend on the specific material, or the setup geometry? If not, should we revise our general understanding of friction based on Amontons' laws? Yet Amontons' laws have worked quite well for centuries so they should still be valid at least in an average sense or in some conditions. All these questions require further theoretical insight and more experiments in mesoscale friction.

V. A FEW SPECIAL FRICTIONAL PHENOMENA

A. Electronic friction

As many theorists (Schaich and Harris, 1981; Persson and Volokitin, 1996; Goncalves and Kiwi, 1999; Novotny and

Velicky, 1999; Plihal and Langreth, 1999; Persson, 2000b; Sokoloff, Tomassone, and Widom, 2000; Sokoloff, 2002b; Volokitin, Persson, and Ueba, 2007) have discussed, sliding friction over a metallic substrate should elicit electronic excitations, giving rise to additional frictional dissipation besides that due to phonons. Thus, for example, friction on a metal surface should drop when the metal is cooled below the superconducting critical temperature, as normal electron-hole gapless excitations disappear. A first QCM report of this frictional drop for the sliding of molecular N_2 islands on a Pb surface (Dayo, Alnasrallah, and Krim, 1998) broke the ice, but also triggered considerable debate (Krim, 1999; Renner, Rutledge, and Taborek, 1999; Fois *et al.*, 2007). Recently, electronic friction was demonstrated in doped semiconductors, where local carrier concentration was controlled through application of forward or reverse bias voltages between the AFM tip and the sample in the *p* and *n* regions, thus demonstrating the capability to electronically tune friction in semiconductor devices (Park *et al.*, 2006).

More recently, using a pendulum-type AFM probe, a clear noncontact friction drop over the surface of Nb was characterized at the superconducting transition (Kisiel *et al.*, 2011). The features observed at this transition follow quite closely the predictions by Persson and collaborators; see Fig. 13. This ultrasensitive pendulum probe is now ready to be put to work to detect the change of electronic friction at other superconducting transitions. The main progress to be expected is now experimental, more than theoretical. Promising cases should include the high-T_c cuprates (Damascelli, Hussain, and Shen, 2003), organics (Kanoda, 2006), fullerides (Gunnarsson, 2004; Capone *et al.*, 2009), heavy-fermion compounds (Ernst *et al.*, 2010), and pnictides (Yin *et al.*, 2009). One interesting physical issue that these
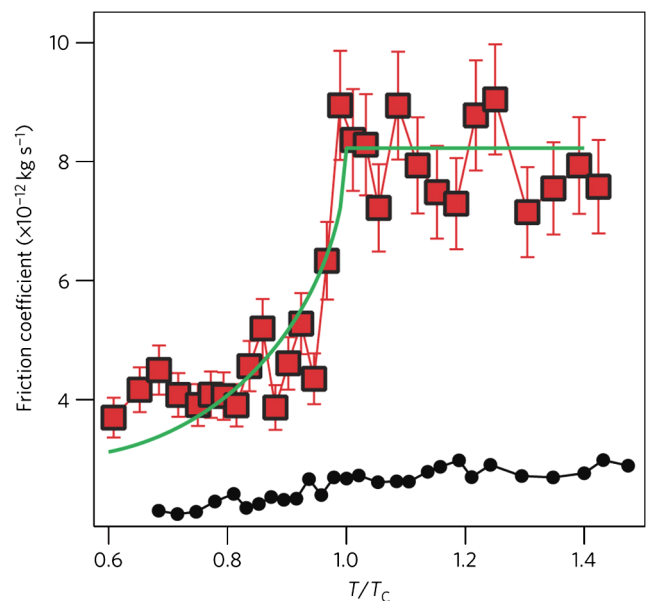

FIG. 13 (color online). Temperature variation of the friction coefficient across the critical point $T_c = 9.2$ K of Nb. Squares and dots: tip-sample separation 0.5 nm/several μm (free cantilever). Solid line: fit by the analytic dependency expected from the Bardeen-Cooper-Schrieffer theory. The friction coefficient is shifted vertically by 2.5×10^{-12} kg s^{-1}. From Kisiel *et al.*, 2011.

investigations could address is the nature and role of strong electron correlations, generally believed to be important for superconductivity in most of these materials. Strongly correlated superconductivity models generally imply that, when not superconducting, the metal is not always Fermi-liquid-like, therefore with vanishingly small quasiparticle strengths and Drude weights. Moreover, it should be noted that a recent experimental and theoretical study demonstrated the general existence at a strongly correlated metal surface of an insulating ''dead layer'' with a thickness which, for example, in V_2O_3 reaches several nanometers (Borghi, Fabrizio, and Tosatti, 2009; Rodolakis *et al.*, 2009). Another interesting case to be studied could be two-dimensional metal-insulator transitions at some surfaces, such as the Mott transition reported for Sn/Si(111) $\sqrt{3} \times \sqrt{3}$ (Modesti *et al.*, 2007; Profeta and Tosatti, 2007).

B. Magnetic dissipation

The relationship between nanofriction and magnetism at the atomic level is an intriguing side direction. In a recent magnetic exchange force microscopy (MExFM) experiment (Wiesendanger, 2009), atomic force sensitivity to the magnetic state of a surface atom was demonstrated for an atomically sharp Fe magnetic tip over the (001) surface of antiferromagnetic NiO (Kaiser, Schwarz, and Wiesendanger, 2007). Besides a different force for the two oppositely polarized surface Ni atoms—well explained by the Fe-Ni exchange available from electronic structure calculations (Momida and Oguchi, 2005)—the results show a surprising difference of mechanical dissipation, with a large excess of order 15–20 meV per cycle in the antiparallel Fe-Ni spin configuration, as compared to the parallel one. The Fe-Ni exchange energy is higher in the antiparallel case, and the difference can clearly be dissipated by flipping the Ni spin. However, direct excitation of surface antiferromagnetic magnons in the antiparallel tip-Ni case—the first obvious possible explanation—is ruled out since, owing to strong dipolar anisotropy, the antiferromagnetic spin-wave dispersion of NiO has a gap $\Delta \sim 1.5$ meV ~ 0.36 THz (Hutchings and Samuelse, 1972) in bulk, and one at least as large at the surface. The low-frequency oscillatory perturbation exerted by the tip (~ 160 kHz) on the surface spin, far smaller than this gap, is completely adiabatic, and direct dissipation in the spin-wave channel is impossible. Other strictly magnetic dissipation mechanisms involving mesoscopic scale phenomena, such as domain wall motion (Liu, Ellman, and Grutter, 1997), also appear inefficient in the atomic scale tip-sample magnetic dissipation. One is left with magnetic coupling to surface atomic displacements. Acoustic phonons are not gapped, both in bulk and at the surface, so they could indeed dissipate. However, the probe frequency is extremely low; and since dissipation vanishes in linear response theory as a high power of frequency (Persson *et al.*, 1999), a magnetic dissipation mechanism via phonons must involve some hysteretic phenomena far from linear response. Recent theoretical work (Pellegrini, Santoro, and Tosatti, 2010) suggests that the nonlinear response may be related to the attainment of a strong coupling overdamped spin-phonon state very well known in other contexts (Caldeira and Leggett, 1981),

giving rise to an unusual kind of single-spin hysteresis. The tip-surface exchange interaction couples together spin and atom coordinates, leading to a spin-phonon problem with Caldeira-Leggett type dissipation. In the overdamped regime, that coupled problem can lead to a unique single-spin hysteretic behavior with a large spin-dependent dissipation, even down to the very low experimental tip oscillation frequencies, just as is seen experimentally. A quantum phase transition to an underdamped regime with a loss of hysteresis and a dramatic drop of magnetic tip dissipation should in principle be found by increasing and tuning the tip-surface distance. This experimental check would also help distinguish this interesting spin-phonon mechanism from more trivial possibilities, such as additional dissipation simply due to a closer distance Fe tip-NiO surface approach in the antiparallel spin configuration.

C. Carbon nanotube friction

Carbon and carbon nanotubes (CNTs) are widely employed in tribology (Chen *et al.*, 2003). Nanotube applications are also numerous in nanofriction. Falvo *et al.* (1999) and also Buldum and Lu (1999) discussed the possibility to slide or roll nanotubes on a surface. Recently, a large longitudinal-transverse anisotropy of AFM friction on surface-deposited CNTs has been explained precisely by the contrast between the longitudinal tube rigidity, against the transverse softness manifested by ''hindered rolling'' (Lucas *et al.*, 2009).

Zettl and collaborators (Cumings and Zettl, 2000; Kis *et al.*, 2006) demonstrated ultralow friction experienced by coaxially sliding multiwall CNTs. Coaxial CNT sliding also inspired numerous simulations (Servantie and Gaspard, 2003, 2006a, 2006b). More simulations identified curious, even if at present rather academic, frictional peaks at selected sliding speeds (Tangney, Cohen, and Louie, 2006) corresponding to the parametric excitation of quantized nanotube breathing modes. Recent theoretical work (Zhang *et al.*, 2009) also discovered that the twofold degeneracy of the breathing modes can cause chiral symmetry to break dynamically at these frictional peaks, so that even purely longitudinal coaxial sliding of nonchiral tubes can generate angular momentum. Other mechanical and rheological properties of CNTs have also been probed by AFM (Palaci *et al.*, 2005).

Water wetting and the interfacial friction of water in CNTs have also been studied for various purposes. The observation of flow-generated voltages growing logarithmically with velocity of ion-rich water (Ghosh, Sood, and Kumar, 2003) appears to be a manifestation of electronic friction which has found various explanations including stick-slip motion of ions embedded in high viscosity water near the tube (Persson *et al.*, 2004) or a statistical consequence of the flow-induced asymmetry in the correlation of the ions, in the ambient fluid as seen by the charge carriers in the CNT (Ghosh *et al.*, 2004).

Recent studies have focused on disentangling confinement and curvature effects on water friction inside and outside CNTs, showing that the friction coefficient exhibits a strong curvature dependence. While for a flat graphene slab friction is independent of confinement, it decreases with CNT radius
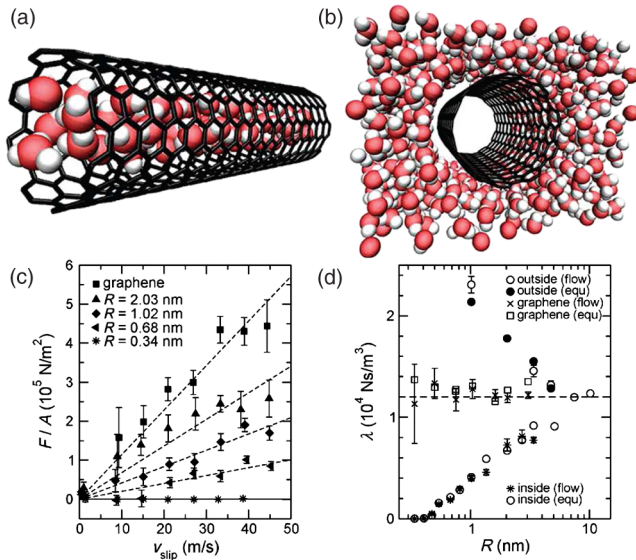
FIG. 14 (color online). Simulated flow of water (a) inside or (b) outside armchair CNTs, and the ensuing friction dependency on (c) slip velocity and (d) confinement radius R. F_k is the kinetic friction force, and λ is the friction coefficient. (c) and (d) include data for graphene slabs, for which $2R$ is the wall-to-wall distance. Adapted from Falk *et al.*, 2010.

for water inside, but increases for water outside; see Fig. 14. The friction coefficient is found to vanish below a threshold diameter for armchair CNTs. A "superlubric," structural origin of this curvature dependence associated with a curvature-induced incommensurability between the water and carbon structures, has been proposed (Falk *et al.*, 2010).

D. Friction in colloidal systems

Handling matter with static periodic fields generated by interfering lasers adds to the realm of toy systems that display real physics. Trapping and handling colloidal particles with intense photon fields offers the possibility to change parameters freely, to compare directly experiment with theory, to test theoretical predictions, and to visualize directly in simple cases the intimate mechanics of sliding friction (Vanossi, Manini, and Tosatti, 2012; Vanossi and Tosatti, 2012). In the novel approach inaugurated by Bechinger's group (Bohlein, Mikhael, and Bechinger, 2012), a 2D close-packed crystal of charged colloidal particles is forced to slide by Stokes forces in the presence of a laser-generated static potential. Unlike conventional sliding crystal surfaces, two-dimensional lattices with different symmetries, lattice spacings, and corrugation amplitudes can be constructed at will, realizing, for example, commensurate or incommensurate matchings, quasicrystal substrate geometries, and possibly "disordered" geometries too.

Besides and above all that, colloidal friction provides an unprecedent real-time visualization of the full frictional dynamics at play. Unlike AFM, SFA, and QCM which provide crucial but averaged frictional data such as the overall static and kinetic friction, mean velocities, slip times, etc., the colloidal experiments photograph the actual time-dependent motion of every individual particle during sliding, an

exquisite privilege restricted so far to the ideal world of MD simulations. Transitions between different dynamical states become experimentally accessible and can be analyzed and related to the detailed particle motion; see, e.g., Reichhardt and Olson Reichhardt (2011) and Bohlein and Bechinger (2012). These and other opportunities lie in the future.

VI. CONCLUSIONS

Among provisional conclusions of this Colloquium, we mention the following:
  (i) Despite limitations, all levels of modeling and simulation are highly informative and predictive.
  (ii) The PT model is, despite its deceiving simplicity, extremely useful in understanding many aspects of nanofriction. Its extreme success tends however to hide the actual complexity of the phenomenon.
  (iii) Multicontact models are instrumental in describing mesoscopic friction and fracture. One main problem of these models is the multiplicity of empirical parameters they involve. Other open problems are under what conditions these models yield realistic stick-slip friction as opposed to smooth sliding, and the exact role of the elastic interactions between contacts.
  (iv) Molecular-dynamics simulations are good and informative for qualitative descriptions of atomic stick-slip motion. Open problems are the high speed of observed change from stick-slip to smooth sliding; the potential artifacts introduced by unrealistic dissipation mechanisms of Joule heat, and more importantly the simulation size and time limitations, in particular, the complete omission of slow, logarithmic relaxations and aging.
  (v) Prospective mechanisms for the control of friction, such as mechanical oscillations or a phase transition in the substrate, are suggested by model studies, and are presently under experimental scrutiny.

It is worth mentioning in closing that there remain fully open problems at the basic theoretical level. First, we do not have a proper theory of friction, namely, a theory where the frictional work could be calculated quantitatively (not just simulated) in all cases—they are the majority—where linear-response theory is inapplicable. Second, while MD simulations can to some extent be used in lieu of theory, they have been so far strictly classical. Future work should include quantum effects and gauge their importance.

There are many more outstanding challenges left in nanofriction. Among them are the following:
  • Bridging the gap between nanoscale and mesoscale (macroscale) friction: multicontact systems.
  • Mechanical control of friction in multicontact systems.
  • The aging of surface contacts at the nanoscales and macroscales.
  • Role of wear and adhesion at the nanoscale.
  • Rolling nanofriction: besides the known case of nanotubes, does it exist, and how can we distinguish between rolling and sliding?
  • Friction in dislocations and in granular systems.
  • Friction in biological systems (motor proteins, cell membranes and pores, etc.).

Lively progress along these and newer lines is to be expected in the near future.

REFERENCES

Ala-Nissila, T., W. K. Han, and S. C. Ying, 1992, Phys. Rev. Lett. **68**, 1866.

Alava, M. J., P. Nukala, and S. Zapperi, 2006, Adv. Phys. **55**, 349.

Allen, M. P., and D. J. Tildesley, 1991, *Computer Simulations of Liquids* (Oxford University, Oxford, England).

Bardotti, L., P. Jensen, A. Hoareau, M. Treilleux, B. Cabaud, A. Perez, and F. C. S. Aires, 1996, Surf. Sci. **367**, 276.

Barel, I., A. E. Filippov, and M. Urbakh, 2012, J. Chem. Phys. **137**, 164706.

Barel, I., M. Urbakh, L. Jansen, and A. Schirmeisen, 2010a, Phys. Rev. Lett. **104**, 066104.

Barel, I., M. Urbakh, L. Jansen, and A. Schirmeisen, 2010b, Tribol. Lett. **39**, 311.

Barel, I., M. Urbakh, L. Jansen, and A. Schirmeisen, 2011, Phys. Rev. B **84**, 115417.

Bar Sinai, Y., E. A. Brener, and E. Bouchbinder, 2012, Geophys. Res. Lett. **39**, L03308.

Baumberger, T., P. Berthoud, and C. Caroli, 1999, Phys. Rev. B **60**, 3928.

Benassi, A., A. Vanossi, G. E. Santoro, and E. Tosatti, 2010, Phys. Rev. B **82**, 081401.

Benassi, A., A. Vanossi, G. E. Santoro, and E. Tosatti, 2011, Phys. Rev. Lett. **106**, 256102.

Benassi, A., A. Vanossi, G. E. Santoro, and E. Tosatti, 2012, Tribol. Lett. **48**, 41.

Benassi, A., A. Vanossi, and E. Tosatti, 2011, Nat. Commun. **2**, 236.

Ben-David, O., G. Cohen, and J. Fineberg, 2010, Science **330**, 211.

Ben-David, O., and J. Fineberg, 2011, Phys. Rev. Lett. **106**, 254301.

Bennewitz, R., A. S. Foster, L. N. Kantorovich, M. Bammerlin, C. Loppacher, S. Schär, M. Guggisberg, E. Meyer, and A. L. Shluger, 2000, Phys. Rev. B **62**, 2074.

Berkovich, R., S. Garcia-Manyes, M. Urbakh, J. Klafter, and J. M. Fernandez, 2010, Biophys. J. **98**, 2692.

Binnig, G., C. F. Quate, and C. Gerber, 1986, Phys. Rev. Lett. **56**, 930.

Bohlein, T., and C. Bechinger, 2012, Phys. Rev. Lett. **109**, 058301.

Bohlein, T., J. Mikhael, and C. Bechinger, 2012, Nat. Mater. **11**, 126.

Bonelli, F., N. Manini, E. Cadelano, and L. Colombo, 2009, Eur. Phys. J. B **70**, 449.

Borghi, G., M. Fabrizio, and E. Tosatti, 2009, Phys. Rev. Lett. **102**, 066806.

Bormuth, V., V. Varga, J. Howard, and E. Schäffer, 2009, Science **325**, 870.

Bouchbinder, E., E. A. Brener, I. Barel, and M. Urbakh, 2011, Phys. Rev. Lett. **107**, 235501.

Bowden, F. P., and D. Tabor, 1950, *The Friction and Lubrication of Solids* (Oxford University, New York).

Braiman, Y., J. Baumgarten, J. Jortner, and J. Klafter, 1990, Phys. Rev. Lett. **65**, 2398.

Braun, O. M., I. Barel, and M. Urbakh, 2009, Phys. Rev. Lett. **103**, 194301.

Braun, O. M., A. R. Bishop, and J. Röder, 1997, Phys. Rev. Lett. **79**, 3692.

Braun, O. M., and Y. S. Kivshar, 2004, *The Frenkel-Kontorova Model: Concepts, Methods, and Applications* (Springer-Verlag, Berlin).

Braun, O. M., N. Manini, and E. Tosatti, 2013, arXiv:1301.4324v1 [Phys. Rev. Lett. (to be published)].

Braun, O. M., and A. G. Naumovets, 2006, Surf. Sci. Rep. **60**, 79.

Braun, O. M., M. V. Paliy, J. Röder, and A. R. Bishop, 2001, Phys. Rev. E **63**, 036129.

Braun, O. M., and J. Röder, 2002, Phys. Rev. Lett. **88**, 096102.

Braun, O. M., and E. Tosatti, 2009, Europhys. Lett. **88**, 48003.

Braun, O. M., A. Vanossi, and E. Tosatti, 2005, Phys. Rev. Lett. **95**, 026102.

Brenner, D. W., O. A. Shenderova, J. A. Harrison, S. J. Stuart, B. Ni, and S. B. Sinnott, 2002, J. Phys. Condens. Matter **14**, 783.

Brenner, D. W., O. A. Sherendova, and A. Areshkin, 1998, in *Quantum-Based Analytic Interatomic Forces and Materials Simulation*, edited by K. B. Lipkowitz, and D. B. Boyd, Reviews in Computational Chemistry (VCH, New York), p. 213.

Brndiar, J., R. Turanský, D. Dietzel, A. Schirmeisen, and I. Štich, 2011, Nanotechnology **22**, 085704.

Brukman, M. J., G. Gao, R. J. Nemanich, and J. A. Harrison, 2008, J. Phys. Chem. C **112**, 9358.

Bruschi, L., A. Carlin, and G. Mistura, 2002, Phys. Rev. Lett. **88**, 046105.

Buldum, A., and J. P. Lu, 1999, Phys. Rev. Lett. **83**, 5050.

Bureau, L., T. Baumberger, and C. Caroli, 2000, Phys. Rev. E **62**, 6810.

Burridge, R., and L. Knopoff, 1967, Bull. Seismol. Soc. Am. **57**, 341.

Caldeira, A. O., and A. J. Leggett, 1981, Phys. Rev. Lett. **46**, 211.

Campana, C., M. H. Müser, and M. O. Robbins, 2008, J. Phys. Condens. Matter **20**, 354013.

Campana, C., B. N. J. Persson, and M. H. Müser, 2011, J. Phys. Condens. Matter **23**, 085001.

Capone, M., M. Fabrizio, C. Castellani, and E. Tosatti, 2009, Rev. Mod. Phys. **81**, 943.

Capozza, R., S. M. Rubinstein, I. Barel, M. Urbakh, and J. Fineberg, 2011, Phys. Rev. Lett. **107**, 024301.

Capozza, R., and M. Urbakh, 2012, Phys. Rev. B **86**, 085430.

Capozza, R., A. Vanossi, A. Vezzani, and S. Zapperi, 2009, Phys. Rev. Lett. **103**, 085502.

Capozza, R., A. Vanossi, A. Vezzani, and S. Zapperi, 2012, Tribol. Lett. **48**, 95.

Car, R., and M. Parrinello, 1985, Phys. Rev. Lett. **55**, 2471.

Carlson, J. M., and A. A. Batista, 1996, Phys. Rev. E **53**, 4153.

Carlson, J. M., J. S. Langer, and B. E. Shaw, 1994, Rev. Mod. Phys. **66**, 657.

Caroli, C., and P. Nozières, 1998, Eur. Phys. J. B **4**, 233.

Carpick, R. W., and M. Salmeron, 1997, Chem. Rev. **97**, 1163.

Castelli, I. E., R. Capozza, A. Vanossi, G. E. Santoro, N. Manini, and E. Tosatti, 2009, J. Chem. Phys. **131**, 174711.

Chandross, M., C. D. Lorenz, M. J. Stevens, and G. S. Grest, 2008, Langmuir **24**, 1240.

Chandross, M., E. B. Webb, M. J. Stevens, G. S. Grest, and S. H. Garofalini, 2004, Phys. Rev. Lett. **93**, 166103.

Chen, W. X., J. P. Tu, L. Y. Wang, H. Y. Gan, Z. D. Xu, and X. B. Zhang, 2003, Carbon **41**, 215.

Cieplak, M., E. D. Smith, and M. O. Robbins, 1994, Science **265**, 1209.

Cochard, A., L. Bureau, and T. Baumberger, 2003, Trans. Am. Soc. Mech. Eng. **70**, 220.

Coffey, T., and J. Krim, 2005, Phys. Rev. Lett. **95**, 076101.

Cule, D., and T. Hwa, 1996, Phys. Rev. Lett. **77**, 278.

Cumings, J., and A. Zettl, 2000, Science **289**, 602.

Damascelli, A., Z. Hussain, and Z. X. Shen, 2003, Rev. Mod. Phys. **75**, 473.

Dayo, A., W. Alnasrallah, and J. Krim, 1998, Phys. Rev. Lett. **80**, 1690.

Dehlinger, U., 1929, Ann. Phys. (Leipzig) **394**, 749.

de Wijn, A. S., A. Fasolino, A. E. Filippov, and M. Urbakh, 2011, Europhys. Lett. **95**, 66002.

de Wijn, A. S., C. Fusco, and A. Fasolino, 2010, Phys. Rev. E **81**, 046105.

Dienwiebel, M., N. Pradeep, G. S. Verhoeven, H. W. Zandbergen, and J. W. M. Frenken, 2005, Surf. Sci. **576**, 197.

Dienwiebel, M., G. S. Verhoeven, N. Pradeep, J. W. M. Frenken, J. A. Heimberg, and H. W. Zandbergen, 2004, Phys. Rev. Lett. **92**, 126101.

Dieterich, J. H., and B. D. Kilgore, 1994, Pure Appl. Geophys. **143**, 283.

Dietrich, J. H., 1979, J. Geophys. Res. **84**, 2161.

Dietzel, D., C. Ritter, T. Mönninghoff, H. Fuchs, A. Schirmeisen, and U. D. Schwarz, 2008, Phys. Rev. Lett. **101**, 125505.

Dong, Y., D. Perez, A. F. Voter, and A. Martini, 2011, Tribol. Lett. **42**, 99.

Drummond, C., and J. Israelachvili, 2001, Phys. Rev. E **63**, 041506.

Drummond, C., J. Israelachvili, and P. Richetti, 2003, Phys. Rev. E **67**, 066110.

Dudko, O. M., A. E. Filippov, J. Klafter, and M. Urbakh, 2002, Chem. Phys. Lett. **352**, 499.

Dudko, O. K., A. E. Filippov, J. Klafter, and M. Urbakh, 2003, Proc. Natl. Acad. Sci. U.S.A. **100**, 11378.

E, W., W. Q. Ren, and E. Vanden-Eijnden, 2009, J. Comput. Phys. **228**, 5437.

Ernst, S., S. Wirth, F. Steglich, Z. Fisk, J. L. Sarrao, and J. D. Thompson, 2010, Phys. Status Solidi B **247**, 624.

Fajardo, O. Y., and J. J. Mazo, 2010, Phys. Rev. B **82**, 035435.

Falk, K., F. Sedlmeier, L. Joly, R. R. Netz, and L. Bocquet, 2010, Nano Lett. **10**, 4067.

Falvo, M. R., R. M. Taylor II, A. Helser, V. Chi, F. P. Brooks Jr., S. Washburn, and R. Superfine, 1999, Nature (London) **397**, 236.

Fedorenko, A. A., P. L. Doussal, and K. J. Wiese, 2006, Phys. Rev. E **74**, 061109.

Filippov, A. E., M. Dienwiebel, J. W. M. Frenken, J. Klafter, and M. Urbakh, 2008, Phys. Rev. Lett. **100**, 046102.

Filippov, A. E., J. Klafter, and M. Urbakh, 2004, Phys. Rev. Lett. **92**, 135503.

Floria, L. M., and J. J. Mazo, 1996, Adv. Phys. **45**, 505.

Fois, G., L. Bruschi, L. d'Apolito, G. Mistura, B. Torre, F. B. de Mongeot, C. Boragno, R. Buzio, and U. Valbusa, 2007, J. Phys. Condens. Matter **19**, 305013.

Frenkel, D., and B. Smit, 1996, *Understanding Molecular Simulation* (Academic, San Diego).

Frenkel, J., 1926, Z. Phys. **37**, 572.

Frenkel, Ya. I., and T. A. Kontorova, 1938, Phys. Z. Sowjetunion **13**, 1.

Fusco, C., and A. Fasolino, 2004, Appl. Phys. Lett. **84**, 699.

Fusco, C., and A. Fasolino, 2005, Phys. Rev. B **71**, 045413.

Gao, J., W. Luedtke, and U. Landman, 1998, J. Phys. Chem. B **102**, 5033.

Gao, J., W. D. Luedtke, and U. Landman, 1997a, Phys. Rev. Lett. **79**, 705.

Gao, J., W. D. Luedtke, and U. Landman, 1997b, J. Chem. Phys. **106**, 4309.

Garg, A., 1995, Phys. Rev. B **51**, 15592.

Garrison, B. J., and D. Srivastava, 1995, Annu. Rev. Phys. Chem. **46**, 373.

Gauthier, M., and M. Tsukada, 2000, Phys. Rev. Lett. **85**, 5348.

Gerde, E., and M. Marder, 2001, Nature (London) **413**, 285.

Ghasemi, S. A., S. Goedecker, A. Baratoff, T. Lenosky, E. Meyer, and H. J. Hug, 2008, Phys. Rev. Lett. **100**, 236106.

Ghiringhelli, L. M., J. H. Los, A. Fasolino, and E. J. Meijer, 2005, Phys. Rev. B **72**, 214103.

Ghosh, S., A. K. Sood, and N. Kumar, 2003, Science **299**, 1042.

Ghosh, S., A. K. Sood, S. Ramaswamy, and N. Kumar, 2004, Phys. Rev. B **70**, 205423.

Gilmore, R., 1981, *Catastrophe Theory for Scientists and Engineers* (Wiley, New York).

Gnecco, E., R. Bennewitz, T. Gyalog, C. Loppacher, M. Bammerlin, E. Meyer, and H.-J. Güntherodt, 2000, Phys. Rev. Lett. **84**, 1172.

Goncalves, A. L. S., and M. Kiwi, 1999, Phys. Rev. B **60**, 5034.

Granato, E., and S. C. Ying, 2004, Phys. Rev. B **69**, 125403.

Guerra, R., U. Tartaglino, A. Vanossi, and E. Tosatti, 2010, Nat. Mater. **9**, 634.

Guerra, R., A. Vanossi, and M. Ferrario, 2007, Surf. Sci. **601**, 3676.

Gunnarsson, O., 2004, *Alkali-Doped Fullerides: Narrow-Band Solids with Unusual Properties* (World Scientific, Singapore).

Gyalog, T., M. Bammerlin, R. Lüthi, E. Meyer, and H. Thomas, 1995, Europhys. Lett. **31**, 269.

Hammerberg, J. E., B. L. Holian, J. Röder, A. R. Bishop, and S. J. Zhou, 1998, Physica (Amsterdam) **123**, 330.

Heimberg, J. A., K. J. Wahl, I. L. Singer, and A. Erdemir, 2001, Appl. Phys. Lett. **78**, 2449.

Helman, J. S., W. Baltensperger, and J. A. Holyst, 1994, Phys. Rev. B **49**, 3831.

Heslot, F., T. Baumberger, B. Perrin, B. Caroli, and C. Caroli, 1994, Phys. Rev. E **49**, 4973.

Heuberger, M., C. Drummond, and J. N. Israelachvili, 1998, J. Phys. Chem. B **102**, 5038.

Hilzinger, H. R., and H. Kronmüller, 1975, J. Magn. Magn. Mater. **2**, 11.

Hirano, and K. Shinjo, 1993, Surf. Sci. **283**, 473.

Hirano, M., and K. Shinjo, 1990, Phys. Rev. B **41**, 11837.

Hirano, M., K. Shinjo, R. Kaneko, and Y. Murata, 1991, Phys. Rev. Lett. **67**, 2642.

Hoffmann, P. M., S. Jeffery, J. B. Pethica, H. O. Özer, and A. Oral, 2001, Phys. Rev. Lett. **87**, 265502.

Hutchings, M. T., and E. J. Samuelse, 1972, Phys. Rev. B **6**, 3447.

Igarashi, M., A. Nator, and J. Nakamura, 2008, Phys. Rev. B **78**, 165427.

Israelachvili, J. N., 1992, Surf. Sci. Rep. **14**, 109.

Jansen, L., H. Holscher, H. Fuchs, and A. Schirmeisen, 2010, Phys. Rev. Lett. **104**, 256101.

Jeon, S., T. Thundat, and Y. Braiman, 2006, Appl. Phys. Lett. **88**, 214102.

Johnson, P. A., and X. Jia, 2005, Nature (London) **437**, 871.

Johnson, P. A., H. Savage, M. Knuth, J. Gomberg, and C. Marone, 2008, Nature (London) **451**, 57.

Johnson, W. L., and K. A. Samwer, 2005, Phys. Rev. Lett. **95**, 195501.

Kaiser, U., A. Schwarz, and R. Wiesendanger, 2007, Nature (London) **446**, 522.

Kammer, D., V. Yastrebov, P. Spijker, and J. F. Molinari, 2012, Tribol. Lett. **48**, 27 (2012).

Kanoda, K., 2006, J. Phys. Soc. Jpn. **75**, 051007.

Kantorovich, L., 2008, Phys. Rev. B **78**, 094304.

Kantorovich, L., and N. Rompotis, 2008, Phys. Rev. B **78**, 094305.

Kantorovich, L. N., and T. Trevethan, 2004, Phys. Rev. Lett. **93**, 236102.

Kim, W. K., and M. L. Falk, 2009, Phys. Rev. B **80**, 235428.

Kim, W. K., and M. L. Falk, 2011, Phys. Rev. B **84**, 165422.

Kis, A., K. Jensen, S. Aloni, W. Mickelson, and A. Zettl, 2006, Phys. Rev. Lett. **97**, 025501.

Kisiel, M., E. Gnecco, U. Gysin, L. Marot, S. Rast, and E. Meyer, 2011, Nat. Mater. **10**, 119.

Kontorova, T. A., and Y. Frenkel, 1938a, Zh. Eksp. Teor. Fiz. **8**, 89.

Kontorova, T. A., and Y. Frenkel, 1938b, Zh. Eksp. Teor. Fiz. **8**, 1340.

Krim, J., 1996, Sci. Am. **275**, 74.

Krim, J., 1999, Phys. Rev. Lett. **83**, 1262.

Krim, J., 2007, Nano Today **2**, 38.

Krim, J., D. H. Solina, and R. Chiarello, 1991, Phys. Rev. Lett. **66**, 181.

Krim, J., and A. Widom, 1988, Phys. Rev. B **38**, 12184.

Krim, J., P. Yu, and R. P. Behringer, 2011, Pure Appl. Geophys. **168**, 2259.

Krylov, S. Y., J. A. Dijksman, W. A. van Loo, and J. W. M. Frenken, 2006, Phys. Rev. Lett. **97**, 166103.

Krylov, S. Y., K. B. Jinesh, H. Valk, M. Dienwiebel, and J. W. M. Frenken, 2005, Phys. Rev. E **71**, 65101.

Kuipers, L., and J. W. M. Frenken, 1993, Phys. Rev. Lett. **70**, 3907.

Kurkijarvi, J., 1972, Phys. Rev. B **6**, 832.

Labusch, R., 1970, Phys. Status Solidi B **41**, 659.

Lacks, D. J., J. Willis, and M. P. Robinson, 2010, J. Phys. Chem. B **114**, 10821.

Lantz, M. A., D. Wiesmann, and B. Gotsmann, 2009, Nat. Nanotechnol. **4**, 586.

Larkin, A. I., and Y. N. Ovchinnikov, 1979, J. Low Temp. Phys. **34**, 409.

Lewis, L. J., P. Jensen, N. Combe, and J.-L. Barrat, 2000, Phys. Rev. B **61**, 16084.

Li, Q., Y. Dong, D. Perez, A. Martini, and R. W. Carpick, 2011, Phys. Rev. Lett. **106**, 126101.

Li, Q., T. E. Tullis, D. Goldsby, and R. W. Carpick, 2011, Nature (London) **480**, 233.

Li, X., and W. E, 2007, Phys. Rev. B **76**, 104107.

Liu, Y., B. Ellman, and P. Grutter, 1997, Appl. Phys. Lett. **71**, 1418.

Liu, Y., and I. Szlufarska, 2012, Phys. Rev. Lett. **109**, 186102.

Liu, Z., J. Yang, F. Grey, J. Z. Liu, Y. Liu, Y. Wang, Y. Yang, Y. Cheng, and Q. Zheng, 2012, Phys. Rev. Lett. **108**, 205503.

Loppacher, C., R. Bennewitz, O. Pfeiffer, M. Guggisberg, M. Bammerlin, S. Schär, V. Barwich, A. Baratoff, and E. Meyer, 2000, Phys. Rev. B **62**, 13674.

Lorenz, B., and B. N. J. Persson, 2012, J. Phys. Condens. Matter **24**, 225008.

Lorenz, C. D., M. Chandross, and G. S. Grest, 2010, J. Adhes. Sci. Technol. **24**, 2453.

Lorenz, C. D., M. Chandross, J. M. D. Lane, and G. S. Grest, 2010, Model. Simul. Mater. Sci. Eng. **18**, 034005.

Los, J. H., L. M. Ghiringhelli, E. J. Meijer, and A. Fasolino, 2005, Phys. Rev. B **72**, 214102.

Luan, B., and M. O. Robbins, 2004, Phys. Rev. Lett. **93**, 036105.

Luan, B. Q., S. Hyun, J. F. Molinari, N. Bernstein, and M. O. Robbins, 2006, Phys. Rev. E **74**, 046710.

Lucas, M., X. Zhang, I. Palaci, C. Klinke, E. Tosatti, and E. Riedo, 2009, Nat. Mater. **8**, 876.

Luedtke, W., and U. Landman, 1999, Phys. Rev. Lett. **82**, 3835.

Magalinskii, V. B., 1959, Sov. Phys. JETP **9**, 1381.

Maier, S., E. Gnecco, A. Baratoff, R. Bennewitz, and E. Meyer, 2008, Phys. Rev. B **78**, 045432.

Maloney, C. E., and D. J. Lacks, 2006, Phys. Rev. E **73**, 061106.

Manini, N., M. Cesaratto, G. E. Santoro, E. Tosatti, and A. Vanossi, 2007, J. Phys. Condens. Matter **19**, 305016.

Marone, C., 1998, Annu. Rev. Earth Planet. Sci. **26**, 643.

Maruyama, Y., 2004, Phys. Rev. B **69**, 245408.

Mate, C. M., 2008, *Tribology on the Small Scale: A Bottom Up Approach to Friction, Lubrication, and Wear (Mesoscopic Physics and Nanotechnology)* (Oxford University, Oxford, England).

McGee, E., R. Smith, and S. D. Kenny, 2007, Int. J. Mat. Res., **98**, No. 05, 430.

Medyanik, S., W. K. Liu, I.-H. Sung, and R. W. Carpick, 2006, Phys. Rev. Lett. **97**, 136106.

Merkle, A. P., and L. D. Marks, 2007, Philos. Mag. Lett. **87**, 527.

Mishin, Y., A. Suzuki, B. P. Uberuaga, and A. F. Voter, 2007, Phys. Rev. B **75**, 224101.

Mo, Y., K. T. Turner, and I. Szlufarska, 2009, Nature (London) **457**, 1116.

Modesti, S., L. Petaccia, G. Ceballos, I. Vobornik, G. Panaccione, G. Rossi, L. Ottaviano, R. Larciprete, S. Lizzit, and A. Goldoni, 2007, Phys. Rev. Lett. **98**, 126401.

Momida, H., and T. Oguchi, 2005, Surf. Sci. **590**, 42.

Müser, M., 2011, Phys. Rev. B **84**, 125419.

Müser, M. H., 2002, Phys. Rev. Lett. **89**, 224301.

Müser, M. H., 2004, Europhys. Lett. **66**, 97.

Müser, M. H., 2006, in *Computer Simulations in Condensed Matter Systems: From Materials to Chemical Biology Vol. 2*, edited by M. Ferrario, G. Ciccotti, and K. Binder, Lecture Notes in Physics (Springer, Heidelberg), Vol. 704, p. 65.

Müser, M. H., and M. O. Robbins, 2000, Phys. Rev. B **61**, 2335.

Müser, M. H., M. Urbakh, and M. O. Robbins, 2003, Adv. Chem. Phys. **126**, 187.

Negri, C., N. Manini, A. Vanossi, G. E. Santoro, and E. Tosatti, 2010, Phys. Rev. B **81**, 045417.

Nielsen, S., J. Taddeucci, and S. Vinciguerra, 2010, Geophys. J. Int. **180**, 697.

Novotny, T., and B. Velicky, 1999, Phys. Rev. Lett. **83**, 4112.

Palaci, I., S. Fedrigo, H. Brune, C. Klinke, M. Chen, and E. Riedo, 2005, Phys. Rev. Lett. **94**, 175502.

Paolicelli, G., K. Mougin, A. Vanossi, and S. Valeri, 2008, J. Phys. Condens. Matter **20**, 354011.

Paolicelli, G., M. Rovatti, A. Vanossi, and S. Valeri, 2009, Appl. Phys. Lett. **95**, 143121.

Park, J. Y., D. F. Ogletree, P. A. Thiel, and M. Salmeron, 2006, Science **313**, 186.

Pellegrini, F., G. E. Santoro, and E. Tosatti, 2010, Phys. Rev. Lett. **105**, 146103.

Perez, D., Y. Dong, A. Martini, and A. F. Voter, 2010, Phys. Rev. B **81**, 245415.

Persson, B. N. J., 1995, Phys. Rev. B **51**, 13568.

Persson, B. N. J., 2000a, *Sliding Friction, Physical Properties and Applications* (Springer, Berlin).

Persson, B. N. J., 2000b, Solid State Commun. **115**, 145.

Persson, B. N. J., 2001, J. Chem. Phys. **115**, 3840.

Persson, B. N. J., 2006, Surf. Sci. Rep. **61**, 201.

Persson, B. N. J., O. Albohr, U. Tartaglino, A. I. Volokitin, and E. Tosatti, 2005, J. Phys. Condens. Matter **17**, R1.

Persson, B. N. J., and F. Mugele, 2004, J. Phys. Condens. Matter **16**, R295.

Persson, B. N. J., and A. Nitzan, 1996, Surf. Sci. **367**, 261.

Persson, B. N. J., U. Tartaglino, E. Tosatti, and H. Ueba, 2004, Phys. Rev. B **69**, 235410.

Persson, B. N. J., and E. Tosatti, 1994, Phys. Rev. B **50**, 5590.

Persson, B. N. J., and E. Tosatti, 1999, Solid State Commun. **109**, 739.

Persson, B. N. J., E. Tosatti, D. Fuhrmann, G. Witte, and C. Wöll, 1999, Phys. Rev. B **59**, 11777.

Persson, B. N. J., and A. I. Volokitin, 1996, in *Physics of Sliding Friction*, edited by B. N. J. Persson, and E. Tosatti (Kluwer Academic, Dordrecht), p. 253.

Peyrard, M., and S. Aubry, 1983, J. Phys. C **16**, 1593.

Peyrard, M., and M. Remoissenet, 1982, Phys. Rev. B **26**, 2886.

Plihal, M., and D. C. Langreth, 1999, Phys. Rev. B **60**, 5969.

Prandtl, L., 1928, Z. Angew. Math. Mech. **8**, 85.

Prioli, R., A. F. M. Rivas, F. L. Freire Jr., and A. O. Caride, 2003, Appl. Phys. A **76**, 565.

Profeta, G., and E. Tosatti, 2007, Phys. Rev. Lett. **98**, 086401.

Pruttivarasin, T., M. Ramm, I. Talukdar, and H. Haeffner, 2011, New J. Phys. **13**, 075012.

Rapoport, L., Y. Bilik, Y. Feldman, M. Homyonfer, S. R. Cohen, and R. Tenne, 1997, Nature (London) **387**, 791.

Reguzzoni, M., M. Ferrario, S. Zapperi, and M. C. Righi, 2010, Proc. Natl. Acad. Sci. U.S.A. **107**, 1311.

Reichhardt, C., and C. J. Olson Reichhardt, 2011, Phys. Rev. Lett. **106**, 060603.

Reimann, P., and M. Evstigneev, 2004, Phys. Rev. Lett. **93**, 230802.

Remoissenet, M., and M. Peyrard, 1984, Phys. Rev. B **29**, 3153.

Renner, R. L., J. E. Rutledge, and P. Taborek, 1999, Phys. Rev. Lett. **83**, 1261.

Riedo, E., E. Gnecco, R. Bennewitz, E. Meyer, and H. Brune, 2003, Phys. Rev. Lett. **91**, 084502.

Robbins, M. O., and M. H. Müser, 2001, in *Modern Tribology Handbook*, edited by B. Bhushan (CRC Press, Boca Raton, Florida), p. 717.

Rodolakis, F., *et al.*, 2009, Phys. Rev. Lett. **102**, 066805.

Rozman, M. G., M. Urbakh, and J. Klafter, 1996a, Phys. Rev. Lett. **77**, 683.

Rozman, M. G., M. Urbakh, and J. Klafter, 1996b, Phys. Rev. E **54**, 6485.

Rozman, M. G., M. Urbakh, and J. Klafter, 1997, Europhys. Lett. **39**, 183.

Rozman, M. G., M. Urbakh, and J. Klafter, 1998, Phys. Rev. E **57**, 7340.

Rozman, M. G., M. M. Urbakh, J. Klafter, and F.-J. Elmer, 1998, J. Phys. Chem. B **102**, 7924.

Rubinstein, S. M., G. Cohen, and J. Fineberg, 2004, Nature (London) **430**, 1005.

Rubinstein, S. M., G. Cohen, and J. Fineberg, 2006, Phys. Rev. Lett. **96**, 256103.

Rubinstein, S. M., G. Cohen, and J. Fineberg, 2007, Phys. Rev. Lett. **98**, 226103.

Ruina, A., 1983, J. Geophys. Res. **88**, 10359.

Sang, Y., M. Dubé, and M. Grant, 2001, Phys. Rev. Lett. **87**, 174301.

Santoro, G. E., A. Vanossi, N. Manini, G. Divitini, and E. Tosatti, 2006, Surf. Sci. **600**, 2726.

Savage, R. H., 1948, J. Appl. Phys. **19**, 1.

Schaich, W. L., and J. Harris, 1981, J. Phys. F **11**, 65.

Schirmeisen, A., L. Jansen, and H. Fuchs, 2005, Phys. Rev. B **71**, 245403.

Schirmeisen, A., L. Jansen, H. Holscher, and H. Fuchs, 2006, Appl. Phys. Lett. **88**, 123108.

Schirmeisen, A., and U. D. Schwarz, 2009, Chem. Phys. Chem. **10**, 2373.

Scholz, C. H., 1998, Nature (London) **391**, 37.

Servantie, J., and P. Gaspard, 2003, Phys. Rev. Lett. **91**, 185503.

Servantie, J., and P. Gaspard, 2006a, Phys. Rev. B **73**, 125428.

Servantie, J., and P. Gaspard, 2006b, Phys. Rev. Lett. **97**, 186106.

Sheehan, P. E., and C. M. Lieber, 1996, Science **272**, 1158.

Shinjo, K., and M. Hirano, 1993, Surf. Sci. **283**, 473.

Singer, I. L., 1998, MRS Bull. **23**, 37.

Socoliuc, A., R. Bennewitz, E. Gnecco, and E. Meyer, 2004, Phys. Rev. Lett. **92**, 134301.

Socoliuc, A., E. Gnecco, S. Maier, O. Pfeiffer, A. Baratoff, R. Bennewitz, and E. Meyer, 2006, Science **313**, 207.

Sokoloff, J. B., 2002a, Phys. Rev. B **65**, 115415.

Sokoloff, J. B., 2002b, J. Phys. Condens. Matter **14**, 5277.

Sokoloff, J. B., and M. S. Tomassone, 1998, Phys. Rev. B **57**, 4888.

Sokoloff, J. B., M. S. Tomassone, and A. Widom, 2000, Phys. Rev. Lett. **84**, 515.

Steiner, P., R. Roth, E. Gnecco, A. Baratoff, S. Maier, T. Glatzel, and E. Meyer, 2009, Phys. Rev. B **79**, 045414.

Stevens, M. J., and M. O. Robbins, 1993, Phys. Rev. E **48**, 3778.

Stills, S., and R. Overney, 2003, Phys. Rev. Lett. **91**, 095501.

Strunz, T., and F.-J. Elmer, 1998a, Phys. Rev. E **58**, 1601.

Strunz, T., and F.-J. Elmer, 1998b, Phys. Rev. E **58**, 1612.

Stuart, S. J., 2000, J. Chem. Phys. **112**, 6472.

Szeri, A. Z., 2001, in *Modern Tribology Handbook*, edited by B. Bhushan (CRC Press, Boca Raton, FL), p. 384.

Szlufarska, I., M. Chandross, and R. W. Carpick, 2008, J. Phys. D **41**, 123001.

Tangney, P., M. L. Cohen, and S. G. Louie, 2006, Phys. Rev. Lett. **97**, 195901.

Tartaglino, U., I. M. Sivebaek, B. N. J. Persson, and E. Tosatti, 2006, J. Chem. Phys. **125**, 014704.

Tartaglino, U., T. Zykova-Timan, F. Ercolessi, and E. Tosatti, 2005, Phys. Rep. **411**, 291.

Thompson, P. A., and M. O. Robbins, 1990, Science **250**, 792.

Tomassone, M. S., J. B. Sokoloff, A. Widom, and J. Krim, 1997, Phys. Rev. Lett. **79**, 4798.

Tomlinson, G. A., 1929, Philos. Mag. **7**, 905.

Trømborg, J., J. Scheibert, D. S. Amundsen, K. Thøgersen, and A. Malthe-Sørenssen, 2011, Phys. Rev. Lett. **107**, 074301.

Tshiprut, Z., A. E. Filippov, and M. Urbakh, 2005, Phys. Rev. Lett. **95**, 016101.

Tshiprut, Z., A. E. Filippov, and M. Urbakh, 2008, J. Phys. Condens. Matter **20**, 354002.

Tshiprut, Z., S. Zelner, and M. Urbakh, 2009, Phys. Rev. Lett. **102**, 136102.

Urbakh, M., J. Klafter, D. Gourdon, and J. Israelachvili, 2004, Nature (London) **430**, 525.

van Duin, A. C. T., S. Dasgupta, F. Lorant, and W. A. Goddard III, 2001, J. Phys. Chem. A **105**, 9396.

van Erp, T. S., A. Fasolino, O. Radulescu, and T. Janssen, 1999, Phys. Rev. B **60**, 6522.

Vanossi, A., A. Benassi, N. Varini, and E. Tosatti, 2013, Phys. Rev. B **87**, 045412.

Vanossi, A., and O. M. Braun, 2007, J. Phys. Condens. Matter **19**, 305017.

Vanossi, A., N. Manini, F. Caruso, G. E. Santoro, and E. Tosatti, 2007, Phys. Rev. Lett. **99**, 206101.

Vanossi, A., N. Manini, G. Divitini, G. E. Santoro, and E. Tosatti, 2006, Phys. Rev. Lett. **97**, 056101.

Vanossi, A., N. Manini, and E. Tosatti, 2012, Proc. Natl. Acad. Sci. U.S.A. **109**, 16429.

Vanossi, A., J. Röder, A. R. Bishop, and V. Bortolani, 2000, Phys. Rev. E **63**, 017203.

Vanossi, A., J. Röder, A. R. Bishop, and V. Bortolani, 2003, Phys. Rev. E **67**, 016605.

Vanossi, A., and E. Tosatti, 2012, Nat. Mater. **11**, 97.

Verhoeven, G. S., M. Dienwiebel, and J. W. M. Frenken, 2004, Phys. Rev. B **70**, 165418.

Volmer, A., and T. Nattermann, 1997, Z. Phys. B **104**, 363.

Volokitin, A. I., B. N. J. Persson, and H. Ueba, 2007, J. Exp. Theor. Phys. **104**, 96.

Voter, A. F., F. Montalenti, and T. C. Germann, 2002, Annu. Rev. Mater. Res. **32**, 321.

Weiner, S. J., P. A. Kollman, D. T. Nguyen, and D. A. Case, 1986, J. Comput. Chem. **7**, 230.

Weiss, M., and F.-J. Elmer, 1996, Phys. Rev. B **53**, 7539.

Weiss, M., and F.-J. Elmer, 1997, Z. Phys. B **104**, 55.

Wiesendanger, R., 2009, Rev. Mod. Phys. **81**, 1495.

Xu, C. H., C. Z. Wang, C. T. Chan, and K. M. Ho, 1992, J. Phys. Condens. Matter **4**, 6047.

Yin, Y., M. Zech, T. L. Williams, X. F. Wang, G. Wu, X. H. Chen, and J. E. Hoffman, 2009, Phys. Rev. Lett. **102**, 097002.

Yosbizawa, H., and J. Israelachvili, 1993, J. Phys. Chem. **97**, 11300.

Zaloj, V., M. Urbakh, and J. Klafter, 1999, Phys. Rev. Lett. **82**, 4823.

Zhang, X. H., G. E. Santoro, U. Tartaglino, and E. Tosatti, 2009, Phys. Rev. Lett. **102**, 125502.

Zhao, X., S. R. Phillpot, W. G. Sawyer, S. B. Sinnott, and S. S. Perry, 2009, Phys. Rev. Lett. **102**, 186102.

Zykova-Timan, T., D. Ceresoli, U. Tartaglino, and E. Tosatti, 2005, Phys. Rev. Lett. **94**, 176105.

Zykova-Timan, T., D. Ceresoli, and E. Tosatti, 2007, Nat. Mater. **6**, 230.